Using stable water isotopes to partition source water contribution and assess spatio-temporal source water dynamics of wetlands ecosystems in the eastern Canadian Rocky Mountains

by

Julia Mary Ann Haiden Hathaway

A thesis

presented to the University of Waterloo

in fulfillment of the

thesis requirement for the degree of

Master of Science

In

Geography (Water)

Waterloo, Ontario, Canada, 2021

Author's Declaration

I hereby declare that I am the sole author of this thesis. This is a true copy of the thesis, including any required final revisions as accepted by my examiners.

I understand that my thesis may be made electronically available to the public.

Abstract

Subalpine and montane regions of the Canadian Rocky Mountains are expected to experience continued changes in hydrometeorological processes due to anthropogenically-tied climate warming. These regions are important in regulating the global water balance since they contribute a significant amount to annual surface runoff. The major river networks sustained by these catchments provide water to a large portion of people in western Canada and parts of the United States. In such environments, wetlands are important elements of mountain hydrologic systems because of their ability to regulate flow by contributing water to downstream sources. However, these ecosystems are potentially sensitive to changing hydrometeorological conditions and it is not clear how climate trends will affect source water composition. Therefore, an understanding of the contribution of subalpine and montane wetlands to downstream water bodies, and their controlling climatic factors, across space and time remains a major gap in mountain hydrological research.

This thesis addresses these research gaps by using stable water isotope (δ^2H and $\delta^{18}O$) techniques to partition source waters from a subalpine wetland to downstream water bodies and assess evaporative fluxes in wetland surface waters across spatial and temporal scales. Since different source waters have distinguishable isotopic signatures, they can be used in combination with knowledge of climate patterns and landscape characteristics to trace spatiotemporal water movement over catchment and regional scales. Source waters (e.g. rain, snow, groundwater, stream, and surface waters) were sampled and analyzed during the 2018, 2019, and 2020 growing seasons, then combined with historic data from 2012, to determine the relative contribution of wetland source waters to downstream water bodies and determine the influence of evaporative fluxes on wetland surface waters.

Overall, the composition of downstream surface waters followed seasonal patterns and indicated periods of heavy source water mixing. There was strong seasonal dependence on snow meltwater, rainfall, and presumably, glacial meltwater during the pre-, peak, and post- growing seasons, respectively. Snowmelt inputs during the pre- growing season recharged groundwater stores and promoted downstream flow. Transitioning to the peak- growing season, the Burstall Valley relied heavily on rainfall to sustain saturation levels and generate runoff. Finally, inputs from glacial meltwater trigged rapid streamflow during the post- growing season resulting in a greater proportion of downstream surface waters originating from the Burstall Streams. There was

minimal evaporation from Burstall Wetland throughout the growing season as seasonal source waters replaced waters stored within the landscape. However, this was not the case at extensive sites. Instead, evaporation fluxes followed a strong spatiotemporal gradient with stronger d-excess signals at lower elevations during the late summer, indicating greater surface water storage capacity. These results indicate that under certain climate conditions (e.g. drought, warmer temperatures), subalpine and montane wetlands may experience increased water loss or dry out during the late summer months if snowmelt continues to occur earlier in the year prolonging the growing season.

Table of Contents

List of Figures

clarity. The Montane Natural Subregion is represented by circles and the Subalpine Natural Subregion is represented by triangles.

List of Tables

Chapter 1: General Introduction

1.1 Background

Snow dominated mountain catchments are places of high environmental value (biodiversity, water supply, climate feedbacks, etc.), and are experiencing shifts in hydrologic processes largely due to rising global temperatures, a trend tightly coupled with human activity (Penna et al., 2014; Ala-aho et al., 2018). In such environments, wetlands are important ecosystems because of their ability to store water for extended periods of time, thus controlling runoff processes, making them potentially important contributors to downstream water bodies (Šanda et al., 2014). This crucial function is sensitive to climate conditions and biological features, and therefore may behave differently across spatial and temporal scales (Hayashi et al., 2016). Yet, it is currently not clear how climate trends will impact wetland function, or mountain hydrologic systems as a whole. Therefore, identifying the factors that influence wetland hydrologic response to climate change is an important step in understanding the sensitivity of these ecosystems to environmental change, and potential mechanisms for adaptation.

Accurate modeling of hydrologic response to current climate trajectories in mountain settings is complicated due to large climate heterogeneity and lack of data (Immerzeel et al., 2012). Current climate models predict that rising air temperatures in the next few decades will result in earlier onset of snowmelt, increased evaporation, and shifts in dominant precipitation regimes (IPCC, 2013; Cowie et al., 2017). Some of the most pronounced changes are forecasted for foothill catchments, where rising air temperatures may decrease the seasonal freezing elevation, leading to more rain versus snow precipitation and an overall reduction in streamflow (Cowie et al., 2017; Knowles et al., 2015). Similar trends are expected for alpine and subalpine catchments, in that rising temperatures are expected to move peak flows associated with snowmelt earlier in the year, leading to more rain on snow events, and decreased runoff during peak growing seasons (Gleick, 1987; Burn, 1994). These climate projections have implications for mountain wetlands however, individual ecosystem responses are not synchronous over space and time. Therefore, understanding climate impacts on different hydrologic classes of wetlands is critical to assessing vulnerability of particular species or types of wetland ecosystems, and more generally to understanding how the wide range of hydrological and ecological services wetlands provide is likely to change over time (Lee et al., 2015).

The Canadian Rocky Mountains are considered the "water towers" of Canada and store and contribute a significant amount of water annually, making them an important component of the regional water cycle (Hrach, 2019). Rocky Mountains wetlands remain far less impacted by anthropogenic disturbance in comparison to those in the lowlands where water withdrawal, land-use change, and direct destruction have caused substantial losses of wetlands over the past two centuries (Lee et al., 2015). For these reasons, wetlands of the Canadian Rocky Mountains are an important resource for understanding baseline patterns and processes of hydrologic variation over time as a function of climate. A markedly understudied topic in this region is the cumulative effects of elevation, location, and seasonality on the relationship between mixing and mobilization of wetland source waters, and subsequent runoff generation in wetland abundant landscapes. Runoff in mountain catchments is controlled by physiography, climate, and landscape characteristics, and differs from low-lying areas in that infiltration of water is restricted, and groundwater discharges to or near the land surface. Snow dominated glacial valley catchments, which are abundant in the Canadian Rocky Mountains, are often surrounded by slopes and thus, are important in regulating flow depending on slope angle (Mosquera et al., 2016). Localized climate patterns regulate water inputs in the form of snow or rain, and water losses through processes such as evapotranspiration. During the peak growing season, wetlands are almost entirely dependent on precipitation inputs for runoff generation, leaving them particularly vulnerable since surrounding surface and groundwater watersheds are negligible (Winter, 1999; Winter, 2000). Comparing physiography and landscape characteristics, recent literature demonstrates that aspects of landscape characteristics, that is soil and vegetation type, most strongly correlate with runoff coefficient however, most of this supporting research was conducted in warm, low elevation catchments (Mosquera et al., 2016; Bullock and Acreman, 2003). In cold region mountain wetlands, it is expected that elevation, presence of glacial melt, and snowmelt, in addition to landscape characteristics will dictate relative contributions of source waters to downstream bodies (Gurtz et al., 1999). The collective influence of these factors is an increasingly important aspect of global, continental, and regional water cycles, and remains largely understudied in Western Canada.

The South Saskatchewan River Basin drainage area, which encompasses the study area of this research and is shown in Figure 1-1, is an excellent example of a basin where downstream communities directly rely on runoff for drinking water and agricultural production. Glacial and

snow meltwater from alpine and subalpine catchments contributes to summer flow of several major river systems that drain the eastern slopes of the Canadian Rocky Mountains, specifically, the Bow, Red Deer, and North Saskatchewan rivers (Figure 1-1). Together, they support invaluable ecosystems, supply resources for hydroelectricity production, and provide water to over 13 million people who reside in British Columbia, Alberta, Saskatchewan, and Manitoba.

The use of stable water isotopes of hydrogen and oxygen (δ^2H and δ^{18}O) is a proliferating method to understand source water mixing and spatiotemporal variations within wetlands and their broader hydrologic roles. Source waters have distinguishable isotopic signatures, which can be used in combination with knowledge of regional landscape characteristics and climate patterns to determine spatial and temporal trends of water movement within a watershed (England et al., 2019). Interpretation of changes in isotopic signatures of regional and catchment waters can thus provide insights to identify hydrological sources and flow paths under different conditions (e.g. climate, topographic) and offer estimates of residence times (Rodgers et al., 2005). This research is essential to best predict potential shifts in hydrologic processes due to climate change and best inform management plans in future years.
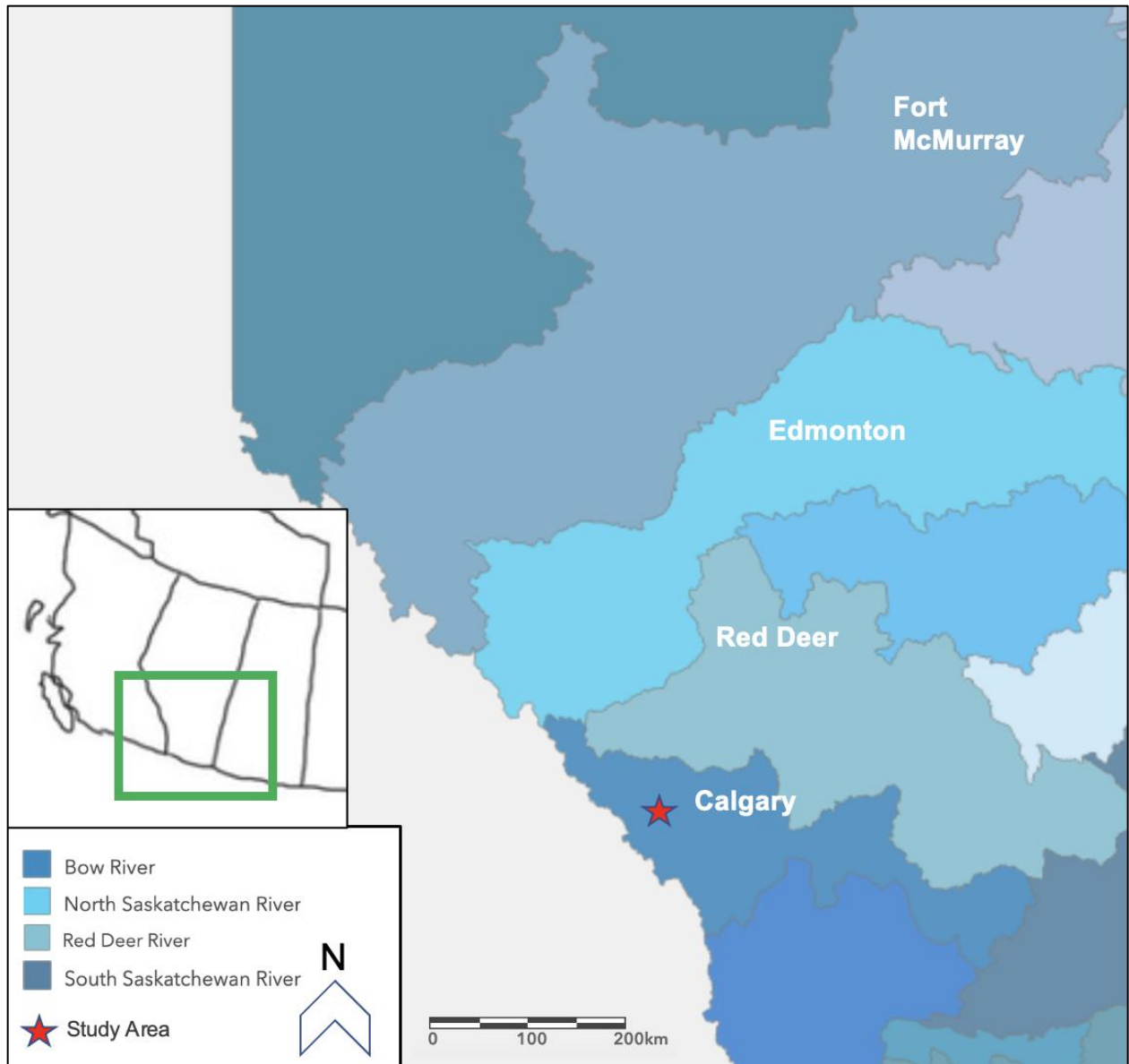
Figure 1-1. Study area within the context of the major watersheds of Alberta. River basins of the South Saskatchewan drainage area (Bow River, North Saskatchewan River, Red Deer River, South Saskatchewan River) and major cities identified. (Data Source: Government of Alberta, Ministry of Environment and Sustainable Resource Development (2011)).

1.2 Research Objectives

Mountain wetlands are increasingly recognized as integral ecosystems in the fight against climate change because of their ability to store and release water, thus providing invaluable protection against natural events such as droughts and floods. In the Canadian Rocky Mountains, the Kananaskis River Valley is positioned on the southern leeward slopes, and discharges water to the greater South Saskatchewan River. The landscape is littered with wetlands, and has therefore been the focus of much wetland hydrometeorological research. Past isotopic studies in the Kananaskis Valley have used δ^2H and $\delta^{18}O$ to investigate snowmelt hydrology, characterize isotope-altitudinal relationships, and partition storm water (Moran et al., 2007; Hopkinson and English, 2001). Yet, an understanding of wetland source water composition throughout the growing season, in the greater context of their importance as contributors to downstream bodies, remains poorly understood. Thus, the general objective of this research is to use δ^2H and $\delta^{18}O$ to provide insights into wetland source water dynamics in a cold region, mountain setting. The results from this study will provide a high-level analysis of mountain wetland source water dynamics, specifically the drivers of downstream flow throughout the growing season, and relevant hydrological processes. This research is important for future management strategies in subalpine and montane regions since it outlines potentially negative hydrologic feedbacks in wetlands due to climate change, some of which are already happening (see Pomeroy et al., 2016). The greater knowledge gained from this study has strong implications for Canada, since these landscapes are prominent in Western regions, and can also be applied in similar international settings. The research objectives of this thesis are divided between two manuscripts. Paper 1 is designed to quantify relative source water contributions to downstream water bodies in a headwater mountain catchment using stable water isotopes δ^2H and $\delta^{18}O$. The objectives of this paper are to: I) partition relative source water contributions from Burstall, a subalpine wetland, to downstream water bodies using a simple hierarchical two component mixing model; and II) determine the relative importance of each source to downstream flow during pre-, peak-, and post growing season. Paper 2 is designed to understand the hydrological processes that influence wetland function within the Kananaskis Valley. The objectives of this paper are to: 1) understand the influence of evaporative fluxes on wetland sites across an elevation range; and II) determine the spatial and temporal variability in wetland source waters (e.g. groundwater, rain, snow, stream, and surface water) over multiple seasons, and the factors influencing them.

Chapter 2: Manuscript 1: Quantifying relative contributions of source waters from a subalpine wetland to downstream water bodies

2.1 Introduction

An evolving grasp of the spatial and temporal dynamics of water origins (i.e., source waters) within mountain headwaters is crucial to our long-term understanding of downstream catchment hydrology given impending changes in hydrological processes. In such environments, wetlands are important ecosystems because they help store and regulate flow, and provide a steady water supply to downstream reservoirs, especially during the late growing season when resources are scarce (Colvin et al., 2019). Such wetlands typically form in valleys via peat accumulation underlain by weathered or fractured bedrock, allowing for infiltration from precipitation and surface waters (Šanda et al., 2014). They experience seasonal hydrologic cycles in which the water budget is comprised of contributions from potential source waters (e.g. groundwater, rain, snow, stream, surface-, and glacial- water). The use of stable water isotopes (δ^2H and $\delta^{18}O$) is an increasingly applied method that can elucidate wetland hydrological dynamics. Variations in stable isotope composition can clarify patterns of groundwater recharge and flow, and have been used to estimate groundwater residence times across diverse landscapes (Rodgers et al., 2005; Liu and Yamanaka 2012). These studies demonstrate that where discrete water inflows can be characterized by distinct isotopic signatures, stable isotopes may indicate the provenance and resident times of wetland waters (Clay et al., 2004). Moreover, isotopic signatures can reflect hydrometeorological conditions providing opportunities to explain source water variation across time and space (Soulsby et al., 2015).

Headwater wetlands are often surrounded by complex landscapes characterized by steep terrain and harsh climates. Such complexities present challenges to water resource managers, especially because estimates of source water mixing and contributions to downstream surface waters cannot easily be directly measured (Pu et al., 2013). Fortunately, end member mixing models parameterized with naturally occurring tracers have proven to be an effective method, used in small-scale catchment studies, to identify the contributions of different components to runoff and evaluate streamflow generation mechanisms (Zhang et al., 2018; Ala-aho et al., 2018; Jin et al., 2012; Maurya et al., 2011; Pu et al., 2013). The modern understanding of both mixing end-members and run-off generation has benefited over the past decades from the increased use

of environmental tracers since different tracers may provide different complementary information (Šanda et al., 2014; Wu et al., 2019; Langs et al., 2020). That is, various biogeochemical tracers and stable isotopes can help curb the sources of runoff and their temporal dynamics (Lessels et al., 2016). The results from end member mixing models can be analyzed to reveal the relative importance of each source water to stimulate water flow both within wetlands and to downstream water bodies. Current knowledge of how relative importance varies as a function of climate may foreshadow potential shifts in source waters in the future and identify how land-use interference impacts mountain wetland hydrologic processes as a whole.

The Canadian Rocky Mountains represent a major source of freshwater in North America since they store and distribute water to millions of people across Western Canada and parts of the United States (Hrach, 2020). The leeward slopes of the Canadian Rockies are littered with subalpine (1300 - 2300 m a.s.l.) and montane (825 – 1850 m a.s.l.) wetlands, all of which are vulnerable to environmental change due to their location in a high-elevation system and reliance on snow and glacial meltwater, creating the ideal sites to study hydrological processes (Reynolds, 2020). This study aims to identify source water contributions and movement to downstream water bodies from a spatiotemporal lens, throughout an exemplar subalpine catchment. Two main objectives will be addressed through the use of δ^2H and $\delta^{18}O$ as tracer inputs to a simple 2-component mixing model in a glacier-fed headwater catchment. The objectives are to: I) partition the relative contribution from the subalpine wetland to downstream water bodies using a simple two component mixing model, and II) determine source waters during pre-, peak-, and end of the growing season over multiple years.

2.2 Materials and Methods

2.2.1 Study Site Description

We used the Burstall Wetland, situated in the Kananaskis region of Alberta on the eastern slopes of the Canadian Rocky Mountains, as a case study to investigate the relative contribution of different water sources to the wetland water budget, and its subsequent contributions to downstream water bodies. Burstall is a mineral wetland stretching about 1.2 km in length with a peat layer extending 20 cm deep. It is poorly drained, with soils resembling peaty muck (Windell et al., 1986).

The Burstall Valley is a steep, glacially carved valley, approximately 6 km long, with the Robertson Glacier occupying the upper 2.8 km (Moran et al., 2007). The Burstall Wetland is positioned at about 1900 m a.s.l. within the low terrain of Burstall Valley (Figure 2-1). There are four lakes at the terminus of the wetland in Burstall Valley - Burstall Lake, Lake 1, Lake 2, and finally, Mud Lake (Figure 2-1). The lakes are fed by precipitation inputs, spring snowmelt and meltwater from the Robertson glacier except Lake 2, which is almost exclusively fed by snow meltwater. Since the upper two lakes act as sediment traps, the influx of sediment entering Lake 2 is restricted, resulting in poor groundwater connectivity (Moran et al., 2007). The hydrology of the valley is controlled by springtime snowmelt water that feeds into the Spray River and subsequently to the Bow River, the major mountain drainage system in southern Alberta (Moran et al., 2007). The wetland vegetation is dominated by *Carex* spp. and *Salix* spp., characteristic of marshes and fens in Alberta.

Typical of most mountain regions in continental locations, the Kananaskis Country climate is highly variable over space and time. Areas like Kananaskis Country, positioned on the leeward slopes are susceptible to easterly, upslope storms that act as classical orographic systems, and are most common in the spring (Stewart et al., 1995). The complex terrain of Kananaskis Country often results in turbulent mixing of air masses due to influences from secondary moisture sources as they cross over topographic barriers (Moran et al., 2007). At higher elevations, most precipitation occurs as snow, and temperatures fluctuate according to variations in the El Nino Southern Oscillation and Pacific Decadal Oscillation (Whitfield, 2014). During the winter months, precipitation is controlled by orographic systems of two major air masses: the maritime Pacific and the continental Polar (Whitfield, 2014). These storms create a

standard elevation relationship (depletion in heavy isotope with altitude), commonly observed on

windward slopes

(Moran et al., 2007).
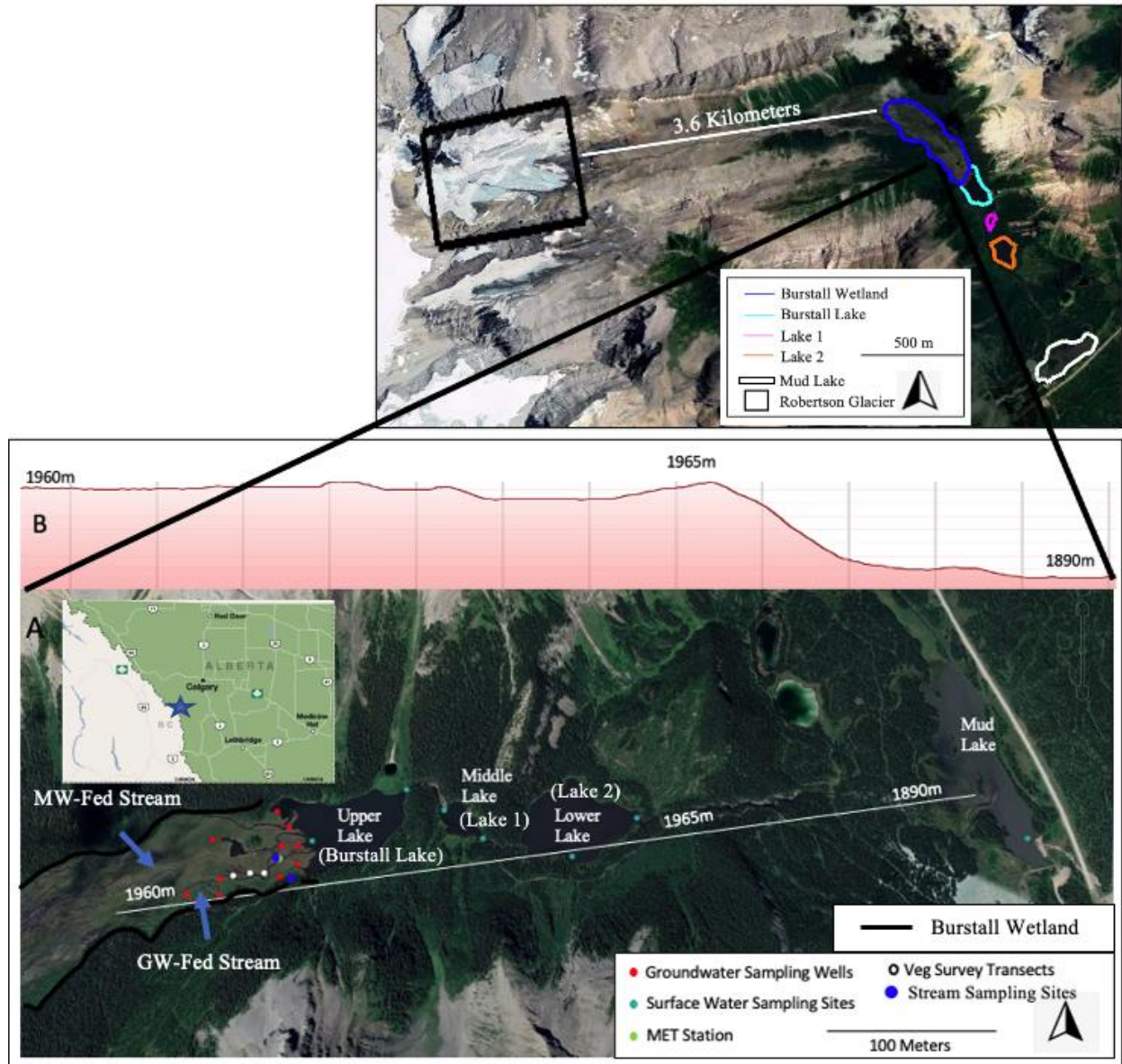
Figure 2-1. Map of Burstall Wetland (A) including sampling locations of groundwater (10) in red, rain (1) in green, snow (1) in green, stream (2) in blue, and surface (7) in teal. The MW-Fed and GW-Fed Streams are identified. Vegetation survey sites are indicated by white (3) dots. The four lakes, including Upper, Middle, Lower, and Mud, are shown and labelled. An approximate outline of the Burstall Wetland is shown in black. The elevation profile line in (A) correlates with the profile in (B). The elevations identified on the profile line (A) are also indicated in the profile in (B) to show the rapid drop after Lower Lake. The greater Burstall Valley is shown in (C) with approximate boundaries of all 4 lakes and the Burstall Wetland outlined. The Robertson Glacier, ranging in elevation from 2504 – 2866 m a.s.l. (Scanlon, 2017), is outlined by a black box. The distance between the terminus of the glacier and the beginning of the Burstall Wetland is 3.6 km.

2.2.2 Hydrometric Data Collection

Wells were hand installed at Burstall Wetland to better understand groundwater movement throughout the wetland and quantify relative contributions of groundwater to downstream water bodies. A total of 11 wells were installed; one near the meteorological (MET) tower (Figure 2-1) at the beginning of the 2019 growing season that was sampled throughout the summer, and the rest were installed at the end of the growing season and were sampled during the 2020 season. Wells were positioned to best reflect both the groundwater- fed (GW- fed) and meltwater- fed (MW-fed) streams, in addition to various ground cover types. Wells were constructed using Schedule 40 PVC pipe slotted along the entire buried length. Fabric 2" diameter well sock (ESP Well Supply, USA) was used to cover the outside surface and act as a screen for fine sediments.

Basic meteorological data was collected by instrumentation on a tripod positioned 4.15 m above the ground near Burstall Lake (Figure 2-1). Relative humidity and temperature were measured with a HMP 155 (Viasala, Finland), as well as rainfall. Rain precipitation was measured at Mud Lake at 2.03m above ground using an Ott Pluvio 400 (Ott Hydromet, CO, USA). The time series for rainfall, temperature, and relative humidity during the study period are provided in Figure 2-2.
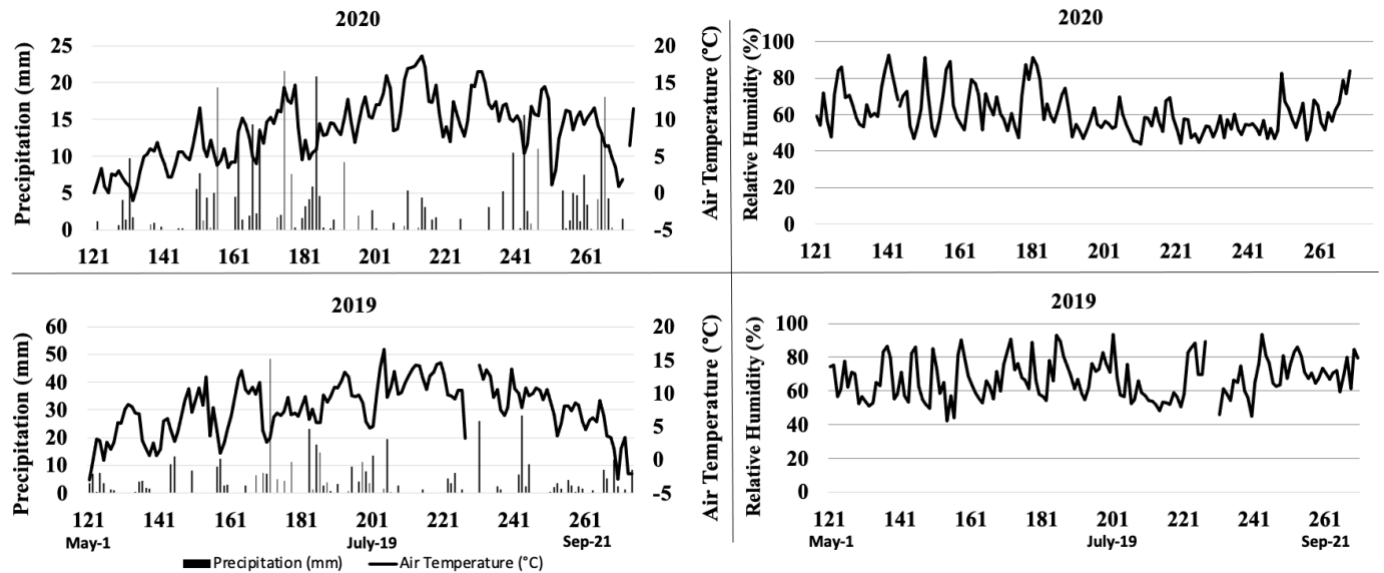
Figure 2-2. Precipitation (mm) plotted from Mud Lake for 2019 and 2020. Air temperature (°C) and relative humidity (%) data plotted from Burstall Wetland for 2019 and 2020 growing season (May-September) shown in 'Day of Year' format.

2.2.3 Vegetation Surveys

Wetland ground cover interferes with the movement of water from rainfall, to groundwater, to runoff generation and is therefore important to consider in wetland hydrological studies. Interferences may occur through processes such as interception, infiltration, or evapotranspiration, all of which can directly alter δ^2H and $\delta^{18}O$ signals from wetland source waters (Le Maitre et al., 1999). Thus, to characterize the groundcover at Burstall Wetland, data from surveys conducted during the summer of 2019 are included to help explain spatiotemporal variation in source water signals.

The ground cover at Burstall Wetland is spatially diverse and varies depending on proximity to a water body (stream or lake). For the purposes of this study, only the four most abundant ground cover species were used to characterize wetland vegetation distribution, the remaining ground cover is identified as "other". Ground cover surveys were carried out across three 50 m transects near the MET tripod (Figure 2-3). The transects were positioned 50 m apart and trended E-W. Along the transects, five 1x1 meter plots were positioned 10 m apart. The percent coverage of all ground cover types were visually estimate for each plot.
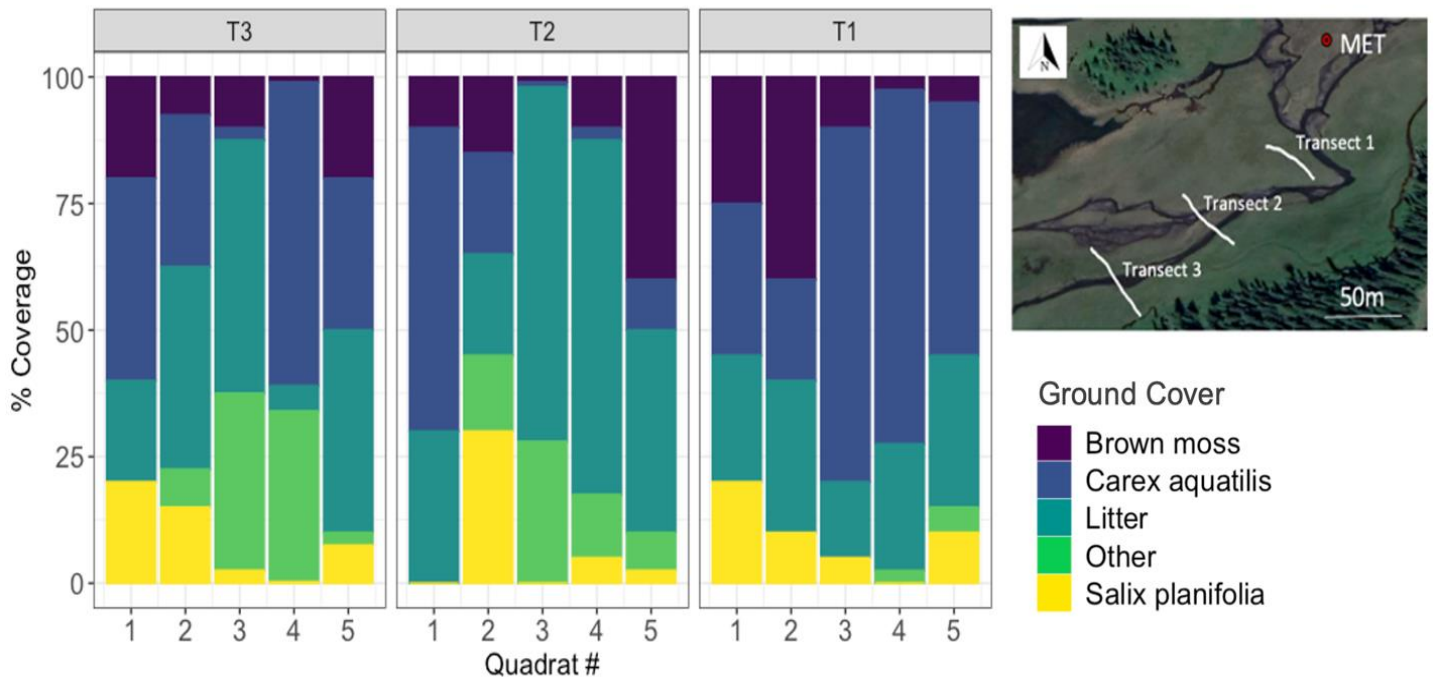
Figure 2-3. Percent cover of the four dominant vegetation types and ground cover at Burstall Wetland shown for three E-W transects. Transect locations are indicated in the map by white lines. The MET tower is included for reference.

The dominant ground cover was *Salix planifolia*, *Carex aquatilis*, brown moss, and litter (Figure 2-3). In this context, litter is defined as dead plant material such as leaves, needles, bark, and twigs. It should be noted, however, that there are distinct patches of *Equisetum hymemale* (horsetail) found only on the eastern edge of the wetland, close to the GW-fed stream.

2.2.4 Isotopic Sample Collection

Potential source waters, including groundwater, rain, snow, stream (GW- and MW- fed), and surface waters were sampled for analysis of δ^2H and $\delta^{18}O$. A summary of δ^2H, $\delta^{18}O$, and d-excess statistics are shown in Table 2-1. Water samples were collected during pre-, peak-, and post growing seasons from May-September in 2019, and during August and September in the 2020 season due to COVID-related access restrictions. Water samples were collected into 20 mL scintillation poly-seal vials with foil lined caps such that the sample contained no headspace. Vials were stored at room temperature (never refrigerated or frozen to limit phase changing) before processing.

During the 2019 field season, groundwater was sampled during the snowmelt period starting in May and lasting throughout the growing season (May-September) at Burstall Wetland. All groundwater sample collection in 2020 occurred only in September. Groundwater samples were taken from wells extending 1 m below ground. Sampling procedures consisted of purging the entire well volume three times before collecting the water sample for stable isotope analysis.

Cumulative rain samples were collected monthly at the Burstall Wetland throughout the 2019 growing season and at the end of the growing season in 2020. The rain collector was positioned near the MET tower and groundwater well (Figure 2-1). Rain collectors were built to collect and limit evaporation of samples between sampling periods (Groning et al., 2012). A plastic hose was watertight sealed to the bottom of a funnel, which was then sealed to the top of a water reservoir container. The hose was cut with enough length to coil on the bottom of the reservoir to ensure the water level of the collected samples topped over the house, limiting evaporation and phase changing of the sample. A ping-pong ball was placed in the top of the funnel to further limit evaporation.

Snow samples were collected for pre- and post- growing season sampling periods when it was present in 2019. Samples were collected using a plastic bag and then were left to melt at room

temperature to ensure complete mixing and no phase change before being sub-sampled into 20 mL poly-seal sampling bottles. The snow was never deep enough to take snow cores so this method was not used. Snow water samples were only collected during the pre- growing seasons on 5 June and 24 June 2019, within 24-hr of the snowstorm. No samples were collected during the 2020 growing season.

Stream samples were collected throughout the 2019 growing season (May-September) at the Burstall Wetland from two different streams, both had water flowing throughout the entire season. We hypothesize that the two streams have different origins based on physical characteristics (e.g. color, location) and were thus each considered a separate source. The MW-fed stream runs through the center of the wetland and consists of clear water during the early summer months, then transitions to cloudy, glacial derived water during the late summer months.

| | | Average | | |
| | | $\delta^{18}O$ | δ^2H | d-excess |
		(‰)	(‰)	(‰)
Pre-	Groundwater	-19.28	-144.16	10.00
	GW-fed Stream	-20.91	-155.59	11.50
	MW-fed Stream	-20.29	-152.36	10.00
	Rain	-18.64	-140.67	8.00
	Snow	-20.08	-151.12	9.33
Peak-	Groundwater	-19.59	-146.40	10.33
	GW-fed Stream	-20.48	-150.79	13.00
	MW-fed Stream	-19.74	-147.70	10.50
	Rain	-18.20	-138.61	7.00
	Snow	N/A	N/A	N/A
Post-	Groundwater	-18.61	-140.49	8.45
	GW-fed Stream	-19.48	-144.84	11.00
	MW-fed Stream	-19.14	-143.22	9.75
	Rain	-15.24	-114.99	6.75
	Snow	-19.66	-145.83	12

Table 2-1. Summary statistics of average $\delta^{18}O$, δ^2H, and d-excess for all source waters from Burstall Wetland. Table is divided into pre-, peak-, and post- growing seasons.

The secondary stream, referred to as GW-fed stream, located on the eastern side of the wetland, consists of reddish-brown water, and is likely groundwater dependent. All 2020 stream samples were collected late in the post- growing season. Samples were taken by dipping uncapped vials into streams facing against the current to ensure minimal hand contact with water sample. Samples were immediately sealed to minimize evaporation.

Surface water samples were collected during September of 2020 at each of the four lakes (Burstall Lake, Lake 1 Outlet, Lake 2 Outlet, and Mud Lake) and Burstall Lake Outlet to measure

movement of source water from one lake to the next. Samples were collected using the same methods described in the paragraph above.

All water samples were analyzed at the Environmental Isotope Laboratory (EIL) at the University of Waterloo, Ontario, using the $\delta^{18}O$ and $\delta^{2}H$ LGR-OA-ICOS Laser System (LGR, 2010; Berman et al, 2013). Quality control was maintained by running a range of water standards including VSMOW (Vienna Standard Mean Ocean Water) and VSLAP (Vienna Standard Light Antarctic Precipitation) from the International Atomic Energy Agency (IAEA). Duplicates were run at a minimum of every fifth samples. Each run also included an in-house check standard for QA/QC of each individual sample batch. Electric conductivity was assumed to be in normal range due to past measurements in the area.

2.2.5 MixSIAR Bayesian Mixing Model

To partition relative source water contributions from Burstall Wetland to downstream water bodies, the R package MixSIAR, a Bayesian mixing model that runs the Markov Chain Monte Carlo (MCMC) method developed by Stock and Semmens (2016), was used. MixSIAR unifies the existing set of mixing model parameterizations into a customizable tool that is designed to analyze biotracer and isotope data to determine relative properties of a mixture and its sources (Stock and Semmens, 2016). The outputs used in this study were summary statistics, which consist of relative contribution percentages and standard deviations, and posterior density plots, which represent the distribution of Bayesian estimated proportions of Burstall Wetland source waters in downstream lakes. Bayesian mixing models improve upon simpler linear mixing models by explicitly taking into account uncertainty in source values, categorical and continuous covariates, and prior-information (Stock and Semmens, 2016). For this study, the script version of MixSIAR was used as the sampling design was a repeated analysis and the MCMC chain lengths could be set. MixSIAR was selected over other mixing model software because of its ability to incorporate covariate data to explain variability in the mixture proportions via fixed and random effects. Different from other Bayesian mixing models, MixSIAR clearly defines and explains the assumed error structures. For the purpose of this study, 'resid_err' was consistently used to account for unexplained deviations from the mean (Stock and Semmes, 2016). MixSIAR assumes mixture values are from a normal distribution, defined by the same mean, with the variance stemming from a combination of source variances (Stock et al., 2018).

14

Five separate model runs were completed, with 3 runs per model, to analyze the combined effects of season and spatial location at different points throughout the catchment. For consistency, each model run had spatial location set as a 'fixed' variable and the time of season was considered a 'random' variable. The MCMC run lengths were set to a chain length of 1,000,000 iterations to ensure the Gelman-Rubin and Geweke statistical diagnostic checks were met and the MCMC chains had converged (Gelman and Ferguson, 2012). Both the tropic enrichment factor and concentration dependence were set to zero.

2.2.6 Data Analysis

Deuterium Excess (d-excess) is associated with kinetic fractionation, which is typically indicative of evaporation or condensation (Ala-aho et al., 2018). Thus, d-excess was used in this study to interpret evaporative and non-evaporative signals across the landscape, and identify meteorological factors associated with different moistures sources throughout the growing season. When d-excess values equal 10, the sample is located on the Global Meteoric Water Line (GMWL). Samples with values <10 plot below the GMWL and signal a deviation from equilibrium fractionation conditions, indicating the samples were subject to evaporative influence (Zega et al., 2020). In addition, because of the close relationship between $\delta^{18}O$ and δD in precipitation, values can reflect different environmental characteristics in precipitation moisture sources.

$$\delta D = \delta^2 H - 8 * \delta^{18}O \qquad (1)$$

2.3 Results

2.3.1. Spatiotemporal Isotopic Characteristics of Source Waters

The isotopic composition of source waters to downstream water bodies varied extensively between rain, groundwater, snow, and streams (GW-fed & MW-fed) throughout the 3 sampling periods (pre-, peak-, post- growing seasons). All source water data is plotted in Figure 4 against the GMWL, the Local Meteoric Water Line (LMWL), and the Local Evaporation Line (LEL). The $\delta^{18}O$ of rain varied the most with values ranging from -16.4‰ to -18.64‰, and a mean (± 1 SD) of -17.64 (± 0.87) ‰. δ^2H value ranged from -123‰ to -140.67‰ with a mean (± 1 SD) of -

133.68 (± 7.07) ‰. Rain signals deviated slightly from the GMWL indicating potential differences in source characteristics of moisture, either due to the seasonal change of meteorological conditions over the ocean, or evaporative enrichment in droplets beneath the cloud base.

Snow water samples were only collected after snowstorms occurring on 5 June and 24 June 2019, immediately after storm events. The $\delta^{18}O$ value of snow water ranged from -19.83‰ to -20.4‰ with a mean (± 1 SD) of 20.08 (± 0.293) ‰. δ^2H ranged from -149.32‰ to -154.12‰ with a mean (± 1 SD) of -151.12 (± 2.61) ‰. The June 5 and 24 collection days were preceded by warmer periods with weekly averages of 8.8 °C and 6 °C, respectively.
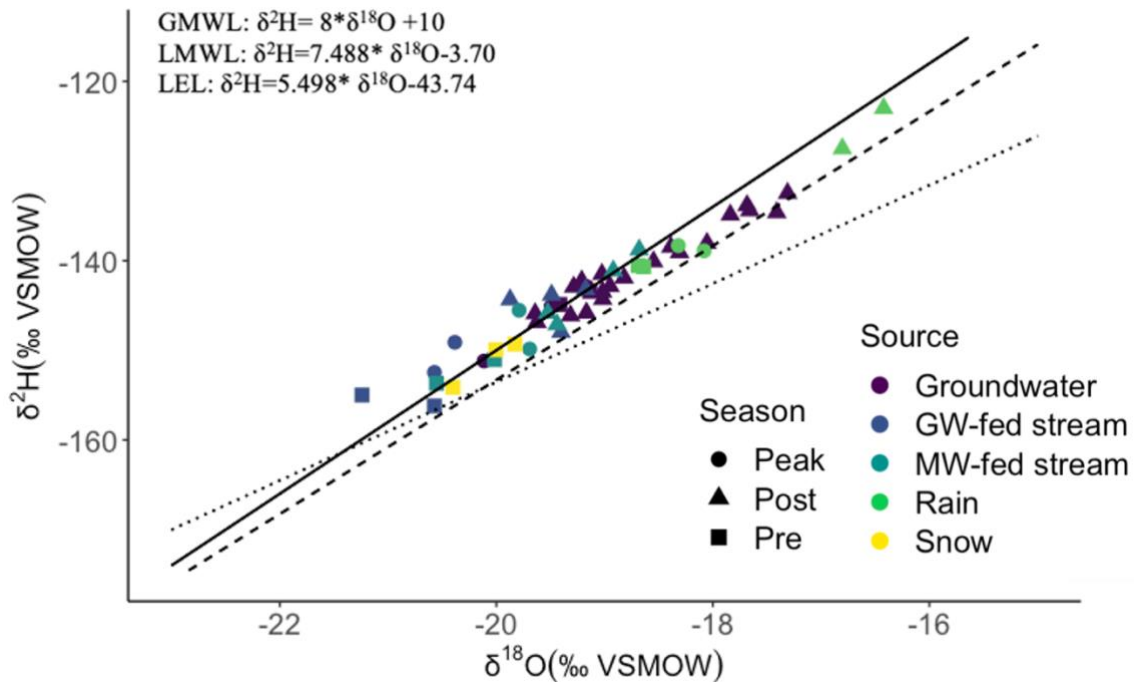
Figure 2-4. Dual isotope plot, depicted by color and shape, of grouped groundwater, rain, snow, and stream (GW-fed and MW-fed) samples collected at Burstall Wetland during the 2019 growing seasons (May-September) and 2020 seasons plotted along the GMWL, LMWL, and LEL. LMWL regression line is $\delta^2H=7.48\delta^{18}-3.70$ (Katvala et al., 2008) with slope falling below the GMWL slope of 8. LEL regression line is $\delta^2H=5.49\ \delta^{18}-62.2$ (Katvala et al., 2008). GMWL shown as $\delta^2H=8\delta^{18}+10$.

Groundwater $\delta^{18}O$ ranged from -17.31‰ to -20.11‰ with a mean (± 1 SD) of -18.78 (± 0.76) ‰. δ^2H value of groundwater ranged from -132.47‰ to -151.19‰ with a mean (± 1 SD) of -141.49 (± 4.74) ‰. The $\delta^{18}O$ values of the GW-fed stream ranged from -19.17‰ to -21.24‰ with a mean (± 1 SD) of -20.08 (± 0.29) ‰. δ^2H ranged from 143.20‰ to -156.20‰ with a mean (± 1 SD) of -149.01 (± 5.11) ‰. The $\delta^{18}O$ values of the MW-fed stream ranged from -18.68‰ to

-20.02‰ with a mean (± 1 SD) of -9.58 (± 0.593) ‰. δ^2H ranged from -138.79‰ to -153.68‰ with a mean (± 1 SD) of -146.62 (± 4.98) ‰. Stream and groundwater are clustered closer to snow than rain, indicating a greater portion of stream and groundwater is snow derived. There are also some groundwater samples taken during the post-growing season deviated from this main cluster, indicating a greater portion of those groundwater samples are rain derived. The overall damped variability among source waters indicates mixing between snowmelt and rainfall with stored waters in the landscape.
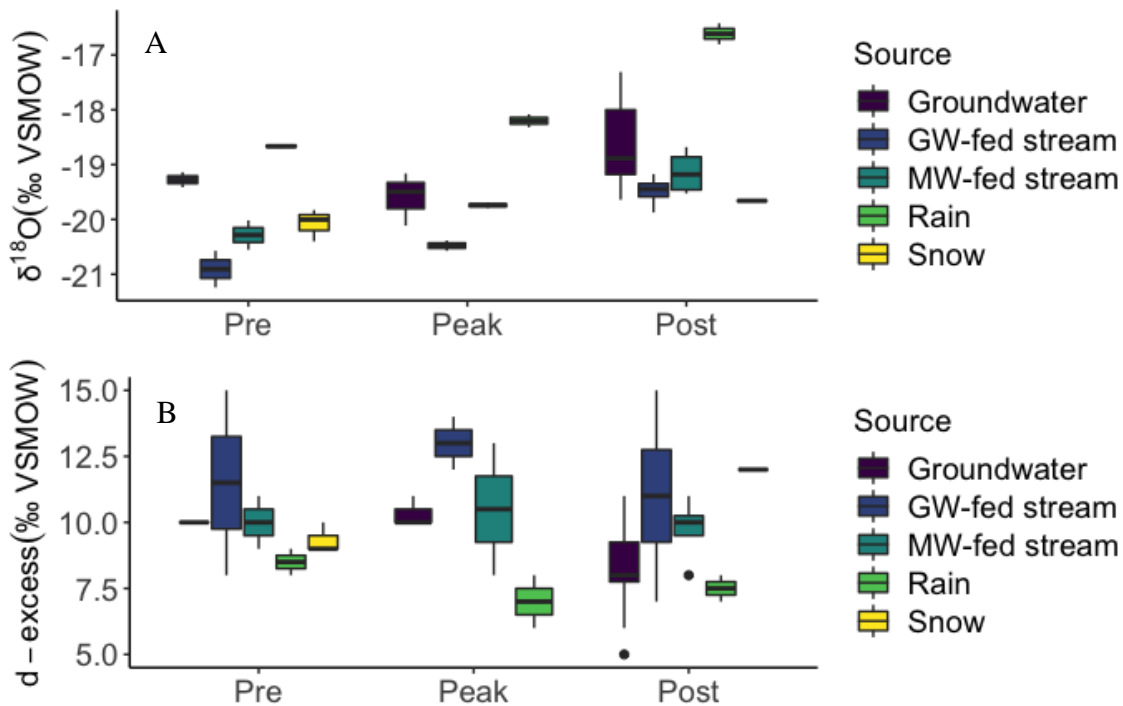
Figure 2-5A&B. $\delta^{18}O$ (A) and d-excess (B) distribution boxplot of source waters depicted by color over the pre-, peak-, and post- growing seasons. D-excess and $\delta^{18}O$ show an inverse relationship indicating that as $\delta^{18}O$ become more enriched, d-excess values are lower.

Groundwater showed significant seasonal enrichment in $\delta^{18}O$ (p = 0.001 when p <0.05 at 95% confidence), consistent with increased temperatures and precipitation throughout the growing season (Figure 2-5A). Both streams exhibited slight enrichment, which is likely the result of rain-enriched inputs, considering the markedly damped variability of d-excess thus minimizing the likelihood of evaporative flux. Interestingly, despite warmer temperatures, the average d-excess values of the GW-fed stream remained above 10% throughout the growing season indicating no significant evaporative influence (Figure 2-5B). The MW-fed stream experienced minimal variations in both $\delta^{18}O$ and d-excess.

The distribution of groundwater $\delta^{18}O$ and d-excess signals varied significantly both seasonally and spatially across Burstall Wetland (Figure 2-5, Figure 2-6). Groundwater samples collected from the middle of the wetland, where peat is >40 cm thick, were more depleted in $\delta^{18}O$ on average than samples collected from the edges (-19.07‰ and -17.74‰, respectively) (Figure 2-6). However, groundwater samples taken from well 3 (Figure 2-6A) did not show depleted $\delta^{18}O$, which was expected given the close proximity to the GW-fed steam, indicating minimal mixing between ground and stream water. Groundwater samples collected in close proximity to wetland margins underwent kinetic fractionation during the post-growing season as indicated by low d-excess values. Samples located near the MW-fed stream had more depleted signatures and greater degree of mixing between groundwater and stream water, which indicates
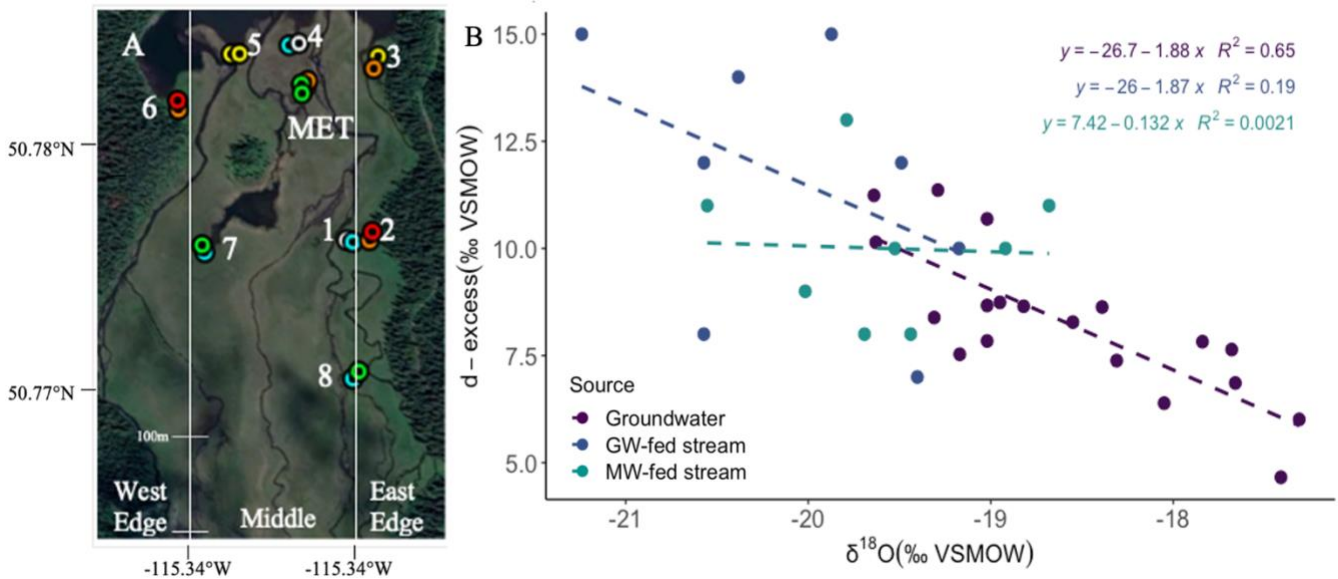
Figure 2-6A&B. Visual distribution of $\delta^{18}O$ values of groundwater throughout Burstall Wetland (A). From depleted to enriched values; red= -17-17.5‰, orange= -17.6-18‰, yellow= -18.1-18.5‰, green= -18.6-19‰, blue= -19.1-19.5‰, and white= -19.6-20‰. Burstall lake is positioned at the top of the map and then extends southward towards Robertson Glacier. (B) Plot of the deuterium excess versus $\delta^{18}O$ for groundwater, GW-fed, and MW-fed streams with regression equations and R^2 values shown.

lateral groundwater movement and stream water infiltration, likely because of the strong presence of *Salix* species in this area (Figure 2-3).

Regression analysis between d-excess and $\delta^{18}O$ of both streams and groundwater was completed to identify mixing between sources to confirm or reject the hypothesis that the GW-fed stream is indeed groundwater-fed. The results do not show clear similarities or overlap in isotopic composition between both sources. Indeed, the GW-fed stream is more isotopically

18

depleted than groundwater, which does not confirm that the GW-fed stream is indeed sourced from groundwater. Figure (2-6B) shows moderate correlation between d-excess and $\delta^{18}O$ (r^2=0.65) in groundwater, indicating that depleted $\delta^{18}O$ corresponds to high d-excess values. The depletion of $\delta^{18}O$ values can be visualized in Figure (2-6A), moving across the wetland from E-W. There was a weak correlation between $\delta^{18}O$ and d-excess in both GW- and MW- fed streams (r^2=0.191, r^2=0.0021, respectively) (Figure 2-6B). In addition, average d-excess values were higher in streams indicating minimal evaporation during the late growing season. Low evaporation and depleted $\delta^{18}O$ confirm the importance of snow melt to stream flow during the spring and glacial melt to stream flow during the peak-post growing seasons.

2.3.2. Relative Source Water Contribution and Dominant Flow Regimes of Burstall Catchment

Results from MixSIAR are separated by location and growing season stage. Location is based on surface water samples collected at the outlet of each lake and are named as follows: Burstall Lake, Burstall Lake Outlet, Lake 1 Outlet, Lake 2 Outlet, and Mud Lake. The exact sampling locations are shown in Figure 1. Growing season stage is partitioned by the sampling events of source waters (groundwater, rain, snow, and stream), into pre-, peak-, and post- growing seasons. The MixSIAR model was run a total of 15 times to partition source waters at each sampling location throughout the 3 growing season stages.

Growing season stage and MixSIAR analysis showed differences across space and time. Although each location had different source water proportions, they all followed similar seasonal trends (Figure 7).

At Burstall Lake, the proportions of source waters during the pre- growing period are as follows: 24% groundwater ($\pm$ 0.195), 41.2% rain ($\pm$ 0.209), 13.7% snow ($\pm$ 0.144), 12% MW-fed stream ($\pm$ 0.135), and 9.2% GW-fed stream ($\pm$ 0.192) (Figure 2-7). The peak- proportions were 25% groundwater ($\pm$ 0.272), 42.8% rain ($\pm$ 0.212), 18.3% MW-fed stream ($\pm$ 0.166), and 13.9% GW-fed stream ($\pm$ 0.123). Finally, post-season proportions were 23.4% groundwater ($\pm$ 0.181), 13.5% rain ($\pm$ 0.006), 18% snow ($\pm$ 0.156), and 23.8% MW-fed stream ($\pm$ 0.176), and 21.4% GW-fed stream ($\pm$ 0.169).

For Burstall Lake Outlet the proportions for the pre- growing period are as follows: 24.4% groundwater ($\pm$ 0.192), 41% rain ($\pm$ 0.093), 13% snow ($\pm$ 0.156), 12.1% MW-fed stream

(± 0.176), and 9.5% GW-fed stream (± 0.169). The peak- proportions were 23.2% groundwater (± 0.1), 46% rain (± 0.094), 17.7% MW-fed stream (± 0.076), and 13.2% GW-fed stream (± 0.053). Finally, peak-season proportions were 23.4% groundwater (± 0.186), 12% rain (± 0.099), 17.6% snow (± 0.15), 24.4% MW-fed stream (± 0.176), and 22.6% GW-fed stream (± 0.164).

Lake 1 Outlet proportions during the pre- growing period are as follows: 23.5% groundwater (± 0.19), 41% rain (± 0.2), 13% snow (± 0.146), 12.1% MW-fed stream (± 0.14), and 10.9% GW-fed stream (± 0.127). The peak- proportions were 19.3% groundwater (± 0.195), 53.9% rain (± 0.236), 15.3% MW-fed stream (± 0.128), and 11.4% GW-fed stream (± 0.101). Finally, post-season proportions were 24% groundwater (± 0.176), 23.1% rain (± 0.116), 14.7% snow (± 0.155), 19.7% MW-fed stream (± 0.173), and 18.5% GW-fed stream (± 0.168).
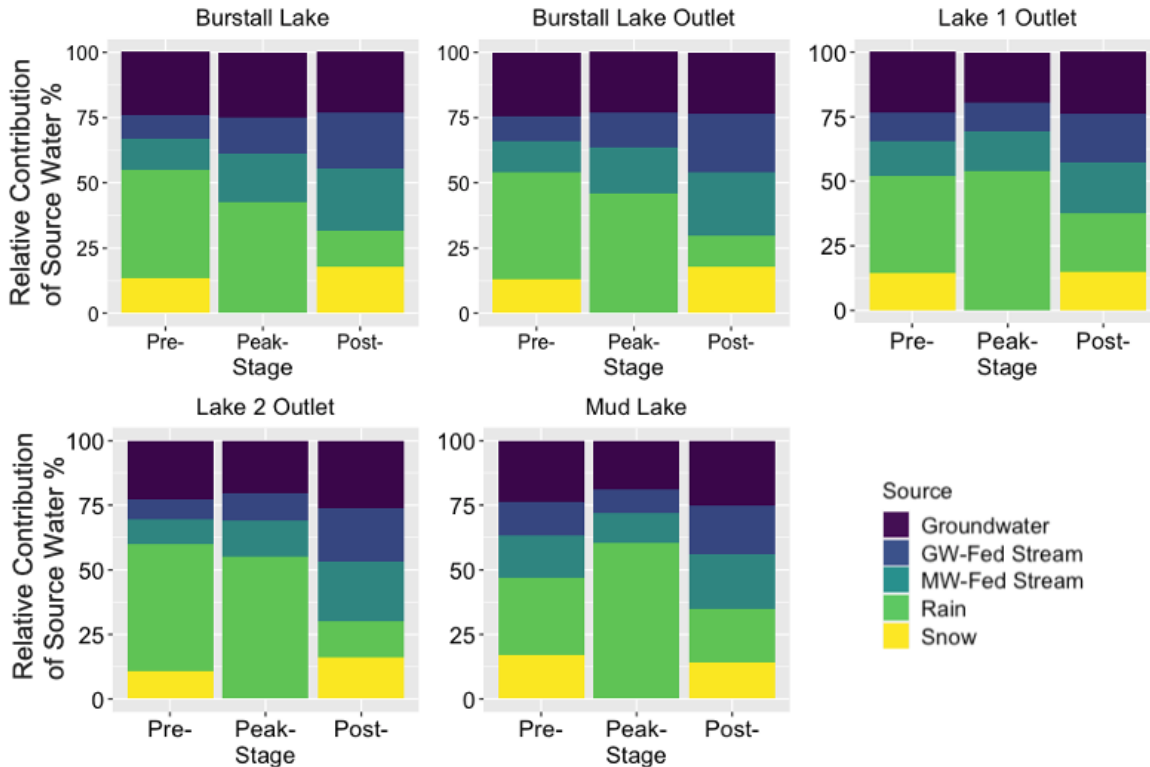
Figure 2-7. Relative source water contribution to downstream water bodies generated by MixSIAR partitioned by sampling period and growing season stage (pre-, peak-, post-).

Lake 2 Outlet proportions during the pre- growing period are as follows: 22.6% groundwater (± 0.202), 49.1% rain (± 0.258), 120.7% snow (± 0.132), 10% MW-fed stream (± 0.133), and 7.5% GW-fed stream (± 0.102) (Figure 2-7). The peak- proportions were 20.3% groundwater (± 0.175), 54.9% rain (± 0.174), 14.4% MW-fed stream (± 0.12), and 10.4% GW-

fed stream (± 0.092). Finally, peak-season proportions were 26.1% groundwater (± 0.16), 14% rain (± 0.183), 16.2% snow (±

Lastly, proportions for Mud Lake for the pre- growing period are as follows: 23.6% groundwater (± 0.188), 29.9% rain (± 0.185), 17% snow (± 0.146), 16.2% MW-fed stream (± 0.149), and 13.3% GW-fed stream (± 0.127) (Figure 2-7). The peak- proportions were 19% groundwater (± 0.197), 60.4% rain (± 0.239), 11.8% MW-fed stream (± 0.124), and 8.8% GW-fed stream (± 0.098). Finally, peak-season proportions were 25.2% groundwater (± 0.19), 20.5% rain (± 0.09), 14.4% snow (± 0.116), 21.4% MW-fed stream (± 0.172), and 18.5% GW-fed stream (± 0.156).

During the pre-growing period, groundwater and rain precipitation were the most readily mobilized, and together comprised the largest portion of source water contribution to each downstream water body (Figure 2-7). During the peak-period, groundwater (37.8%) just barely comprised the largest portion of source water contribution to Burstall Lake, followed by rain (33%), MW-fed stream (17.4%), and GW-fed stream (11.8%) (Figure 2-7). This can be explained by source water mixing at the lake surface and greater reliance on groundwater as the dominant flow source in Burstall Wetland due to less frequent precipitation events and higher mean air temperatures (Figure 2-2). Moreover, during the peak- growing season, snowmelt is likely presenting as groundwater, contributing to a greater proportion of groundwater to downstream water bodies.

Rain was the dominant source water input (69.9%) to Burstall Lake Outlet during the peak-period, controlling surface connectivity between Burstall Lake and Lake 1. Lake 1 Outlet, Lake 2 Outlet, and Mud Lake also saw an increase in rain as the main contributor to source water composition during the peak-growing season (11.6%, 52.7%, 18.8%, respectively) (Figure 2-7). There was a significant increase in stream water contribution during the post-growing season correlated with less rain events and consistent inputs from glacial melt water. Groundwater comprised a relatively small portion of surface water at Lake 2 during the peak- and post-growing seasons, confirming reliance on potential meltwater inputs.

The spatiotemporal consistency in source water composition of surface waters generated by MixSIAR allowed for the development of a generalized schematic representation of water movement throughout Burstall catchment during the pre-, peak-, and post- growing seasons (Figure 2-8). For the purposes of this schematic, the GW-fed and MW-fed stream data was

represented as one group because of the similarity in their relative contributions to downstream water bodies. During the pre-growing season, frequent rain events and meltwater inputs triggered rapid streamflow and groundwater recharge resulting in mixing at lake outlet surfaces (Figure 8). As temperatures increase and meltwater (snow) inputs cease, rain becomes the prevailing source water input, and is quickly mobilized during the peak-growing season reducing water residence time and mobilizing groundwater stores (Figure 2-8). The post-growing season correlated with less rain events and presumed inputs from melt water from the Robertson Glacier. Although rain is the dominant source, total precipitation during August is significantly lower than June (83.2 mm vs. 142.2 mm, respectively), and evaporation is increased due to higher temperatures resulting in lower lake water levels, thus indicating periods of low flow during the peak season. During the post-growing season, MixSIAR shows mixing between stream water, groundwater, and rain as the three become the dominant contributors to surface water composition (Figure 2-7).
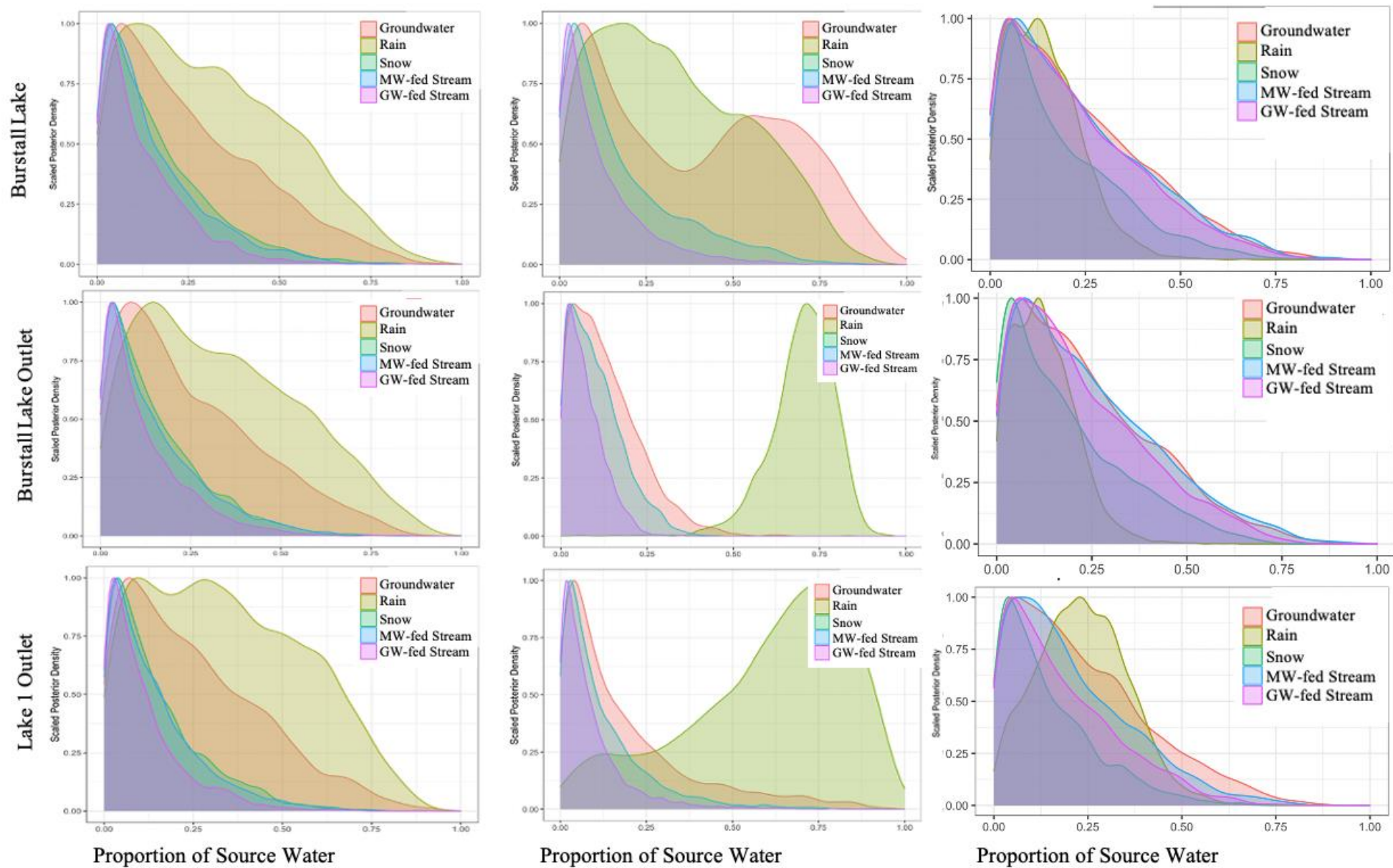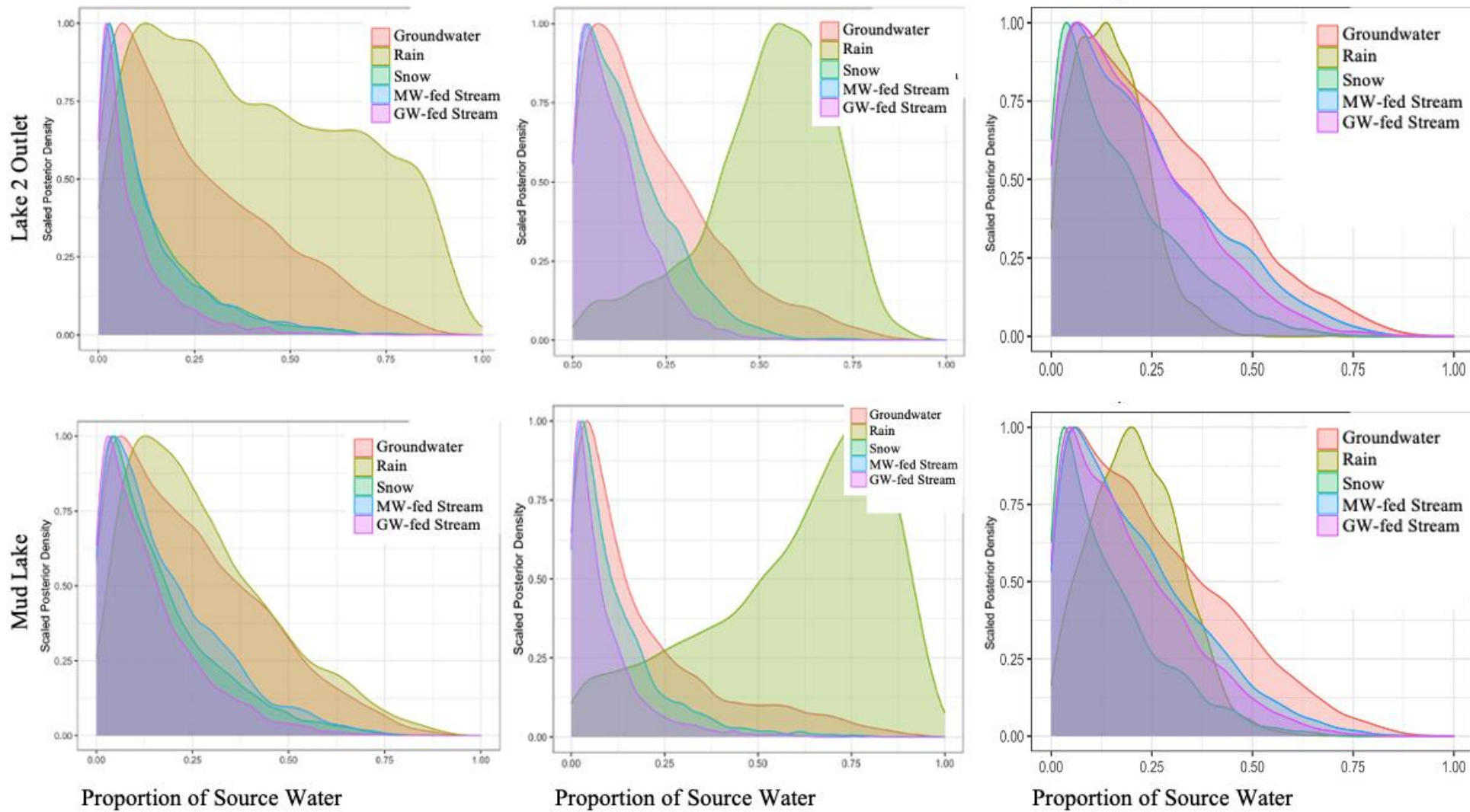
Figure 2-8. Density and proportion spread plots of source water contribution to downstream water bodies generated by MixSIAR for time of growing season (pre-, peak-, post-).
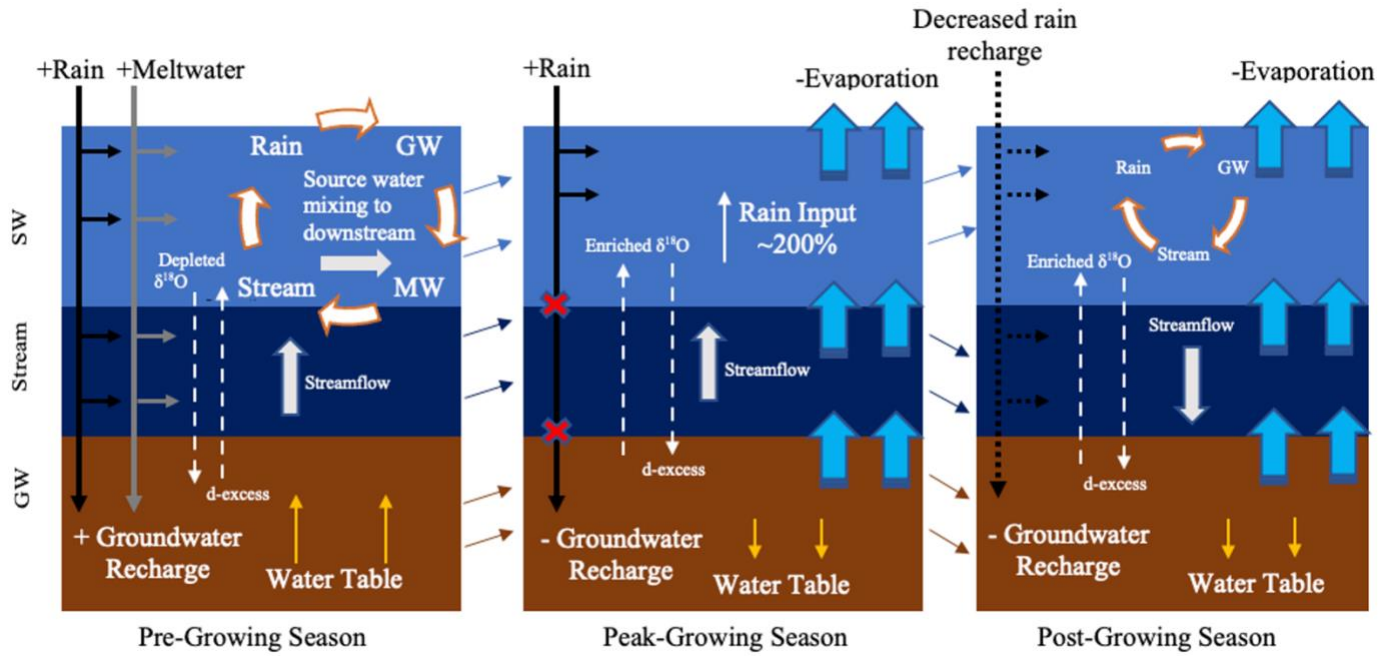
Figure 2-9. Schematic of water movement throughout Burstall Wetland during the pre-, peak-, and post-growing season based on results from MixSIAR (Figure 2-7).

2.4 Discussion

Subalpine wetlands are potentially important elements of mountain hydrologic systems as contributors to downstream water bodies, but due to their remote nature and harsh climate, their hydrology is not well studied. This research addressed the importance of wetlands in mountain hydrologic systems as potential contributors to downstream water bodies, and the processes that influence them across spatiotemporal scales. We applied stable isotope modeling techniques to partition the relative contribution from the subalpine wetland to downstream water bodies using a simple two component mixing model, and determine source waters during pre-, peak-, and end of the growing season over multiple years. Overall, we found that the seasonal patterns in Burstall Wetland water isotopic rations conformed to expectations, reflecting a greater reliance on snowmelt in spring and rainfall in peak and post-growing season periods, when evaporation rates were highest. The variations in source water contributions from MixSIAR analysis provided insights into water movement throughout Burstall Wetland at different stages of the growing season. We found a substantial degree of mixing between precipitation (rain and snow) and stored waters in the landscape, especially during the pre-growing season. This research is important because mountain wetlands are potentially sensitive to climate change (Streich and Westbrook, 2020), and it is not clear how climate trends will affect source water composition.

2.4.1 Differences in Spatiotemporal Water Sources Within Burstall Wetland

The use of stable isotope signatures of $\delta^{18}O$, δ^2H, and calculated d-excess, in combination with MixSIAR results, provides insights into source water origins and relative contributions of the Burstall Wetland to downstream water bodies. Plotted rain data followed an expected seasonal distribution, consistent with low temperatures during the pre-growing season, and warmer temperatures during late August and September. The lower and higher isotopic values of precipitation events are attributed to seasonal changes in meteorological parameters and moisture sources as easterly up-slope conditions prevail, resulting in mixing of air masses at higher elevations. This is evident in Figure 2-5 as the progressive enrichment of $\delta^{18}O$ from the pre- to post- growing season is consistent with a rise in temperatures. The slight decrease in d-excess from the pre- to post- growing season also suggests seasonal meteorological change, and reduces the likelihood of strong evaporative fractionation as the enrichment causation, given that only minor deviations from the GMWL occur (Figure 2-4). Lone et al. (2021) reported similar

seasonal results from a high elevation glacier-fed catchment in which rain exhibited the greatest degree of variability among source waters, and seasonal changes in isotopic composition of rain were tightly correlated with seasonal meteorological changes.

The isotopic composition of groundwater was found to be variable throughout the growing season, both spatially and temporally. The depleted signatures during the pre-growing season are attributed to infiltration and mixing of meltwaters from higher elevations in the Burstall Valley, and from runoff from surrounding uplands. Regardless, the groundwater samples fall between precipitation (rain and snow) indicating that these are major sources of groundwater recharge for Burstall Wetland. At the end of the peak growing season groundwater d-excess dropped, coinciding with a period of little to no precipitation and high temperatures, suggesting water loss from non-equilibrium evaporation and increased evapotranspiration, resulting in water table drawdown. This is a period of low-flow at Burstall Wetland before depleted glacial meltwater inputs penetrate the wetland, lowering the $\delta^{18}O$ content of groundwater. Results also showed considerable spatial variation of the d-excess content within the wetland. The margins of Burstall Wetland support brown moss and *Equisetum hyemale* (horsetail), and are the first areas to dry during summer months (decreased d-excess), while the interior mainly supports densely packed shrubs and grasses (increased d-excess) that remain reasonably wet during summer months (Figure 2-6A). Shrub and grass species produce a much thicker canopy, thus blocking direct radiation to Burstall Wetland surface water, resulting in decreased evaporation rates relative to the wetland edges. Similar results were obtained from a study that used d-excess to assess spatiotemporal variation in isotopic signatures of a wetland, in which results were attributed to solar radiation interception by broad leaf canopies (Zhai et al., 2019). Zhai et al. (2019) reported a strong correlation between the spatial distribution of $\delta^{18}O$ and d-excess values with vegetation coverage; water had lower fractional evaporation in areas of high vegetation coverage compared to areas of low vegetation coverage (Zhai et al., 2019).

Interestingly, the $\delta^{18}O$ composition of stream water remained fairly linear throughout the growing season compared to groundwater, and was overall more depleted. The narrow range compared to groundwater indicates the waters originating from headstreams mixed to give composite stream water. The relatively depleted isotopic value of the GW-fed stream compared to the MW-fed stream could refer to low evaporation rates. Although the d-excess range of the GW-fed stream does widen during the post growing season, it largely remains above the global

average (10‰) therefore indicating minimal evaporation. The observed d-excess could be a result of proximity to the upland, resulting in a degree of canopy coverage and/or unexplained water inputs. The d-excess of the MW-fed stream remains markedly unchanged throughout the growing season due to rapid discharge, common in headwater areas. The rapid discharge results in less transient time of water induced by gradients and shading of downstream water bodies and hence least effect of evaporation/fractionation on stable water isotopes. Overall, if groundwater was the source of the GW-fed stream, we would expect the signals to overlap considerably more than the results show. Thus, we cannot confirm the origin of the GW-fed stream, or that its primary sources differ from that of the MW-fed stream, and recommend further study.

The damped variability of signals within the MW-fed stream indicates mixing and is consistent with results from other studies (Ala-aho et al., 2018; Cao et al., 2018; Lone et al., 2021). Jin et al. (2012) reported similar results from a study conducted in the American Rocky Mountains of seemingly unaffected stream water isotopic composition at the time of snowmelt, when snowmelt presumably provided much of the stream water. They hypothesized that rapid snowmelt releases water with homogenized isotopic value, regardless of stratification during the winter due to increasingly enriched snow fall (Jin et al., 2012). At Burstall, a similar situation could have occurred in which rain on snow events caused mixing, resulting in homogenized waters in streamflow. Indeed, studies confirm that the isotopic composition of precipitation affects that of snowpack outflow and is largely controlled by residence time of liquid water in snowpack (Rucker et al., 2019; Juras et al., 2016). Thus, high magnitude precipitation events occurring during the late spring could cause prolonged residence times and lead to mixing between rain and snow and eventually stream water, creating the resulting damped isotopic values found in this study. However, the effects of rain on snow events are highly variable and further investigation is needed to confirm.

2.4.2 Relative Source Water Partitioning

Stable water isotopes of $\delta^{18}O$ and δ^2H were used as environmental tracers to determine subalpine source water partitioning during three periods in the growing season (pre-, peak-, post-) using MixSIAR. In general, groundwater via snowmelt was an important water source for all lakes, especially during the pre- growing season. Contributions of snowmelt to groundwater, in addition to streams, created considerable mixing in downstream surface waters. The estimated

proportion of rain was greater in all downstream bodies during the pre-growing season, coinciding with high precipitation events, suggesting rain was readily mobilized once it reached the surface. Although, cooler temperatures during the pre-growing season, and influences from snowmelt, clearly affected rain signals because they were still reasonably depleted. The confidence intervals of snow, GW-fed stream, and MW-fed stream were narrow, indicating the true proportion of each source likely lies between 0.0 and 0.25. The posterior density plots do, however, show large uncertainty intervals as to the exact contribution of rain [0.0, 0.8] and groundwater [0.0, 0.8] during the pre-growing season. This could be a result of the range in rain and groundwater source data however, outlier analysis did not reveal any outstanding measurements. Thus, the wide confidence interval could be narrowed by incorporating more consumer or source data (Stock and Semmens, 2008). The relative contribution of both the GW-fed and MW-fed streams are comparable during the pre-growing season, which is expected given the similarities in $\delta^{18}O$ composition of both sources.

Rain was the dominant driver of streamflow generation during the peak-growing season in Burstall Wetland after snowmelt inputs declined. All posterior plots of source water estimate that the true portion of rain is roughly 70%, except Burstall Lake. The Burstall Lake posterior plot is multimodal, which is the result of a relatively high likelihood of multiple scenarios. Thus, the model creates an output to reflect alternative scenarios. To address this, informative priors can help when variability among inputs is not sufficient to identify unimodal posterior distributions, or more consumer or tracer data could be added. The clear period of low rain precipitation during the peak growing season is concerning given the projected occurrence of earlier onsets of spring snowmelt. Longer growing season times may increase evaporation from wetland surface water and groundwater, resulting in a larger summertime water table drop, and greater reliance on rain to stimulate downstream flow.

The post-growing season results indicated that downstream surface waters were well mixed. The relative contribution of rain water decreased and was replaced by an influx of stream water. This is expected since it is well known that streamflow in September is composed largely of meltwater runoff from glaciers, including contributions from both the overlying seasonal snowpack and glacier ice, in the eastern Canadian Rockies (Marshall et al., 2013). In this system, temporal variations of source water proportions were clearly due to differences in snowmelt during the early growing season and glacial melt during the post growing season. Annual

variations in glacial and snow meltwater signatures are likely a result of moisture sources for the area and are subject to change, especially given the location of Burstall Wetland. Similar to other studies conducted in glacial fed, headwater systems, if glacial mass continues to decline as it has in the past several decades, this study suggests that streamflow in the Burstall Valley may decline during critical times, potentially hindering wetland function as a carbon sink (Cable et al., 2011; Mark and Seltzer , 2003).

2.5 Conclusions

There is mounting evidence that wetland hydrological processes in headwater catchments are changing, however, the implications for source water composition is not yet clear (Klein et al., 2005; Lee et al., 2015; Zhang et al., 2016). This research addressed the importance of wetlands in mountain hydrologic systems as potential contributors to downstream water bodies, and the processes that influence them across spatiotemporal scales. Using a stable isotope approach our results revealed significant mixing between source waters during the pre-growing season, indicating that both rain and snow are important components of recharge in the Burstall Valley. The importance of snowmelt as a driver of streamflow generation is widely recognized however, continued warming is projected to alter pre-growing season snow precipitation regimes. Recent studies have linked patterns of earlier spring snowmelt and amplified rain events in mountain catchments to increased warming (Lopez-Moreno et al., 2021; Musselman et al., 2018; Harpold et al., 2017). These occurrences trigger rain-on-snow events, which are responsible for many of the most damaging floods in mountain areas (Pomeroy et al., 2016). In late June of 2013, rapid snowmelt and heavy rainfall triggered flooding throughout much of the southern half of Alberta (Pomeroy et al., 2016). Tributaries to the Bow River, including the Kananaskis, reached flood levels, and wetlands in this region eventually became overwhelmed leading to some damage. Although it is impossible to estimate the exact benefits wetlands provide during such events, it is important to continue to re-evaluate and study ecosystem hydrologic response to best prepare for the future flood events.

During the peak growing seasons, wetlands in snow-dominated landscapes are experiencing earlier drawdowns, accelerated recession rates, and lower minimum water levels as snowpack declines initiate earlier runoff (Ray et al., 2019). This leads to longer growing seasons resulting in greater reliance on rain and presumably, glacial meltwater to maintain downstream

flow. Under these circumstances, consecutive years of drought could put Burstall at risk of significant water loss due to longer growing seasons and increased evaporation rates. This is true for other subalpine headwater catchments that may experience similar shifts in hydrological processes due to continued environmental change.

Manuscript 2: Chapter 3: Using stable water isotopes to analyze spatiotemporal variability and hydrometeorological forcing in mountain valley wetlands

3.1 Introduction

Mountain wetlands are considered to play an important role in regional hydrologic processes that underlie a range of potential ecosystem services. Perhaps some of the most valuable are flood attenuation, water storage, carbon abatement, biodiversity support, and their ability to import and export materials (e.g., sediment, organic matter, nutrients, etc.) (Kadykalo & Findlay, 2016). Anthropogenic climate change is expected to significantly alter hydrologic regimes in montane and subalpine environments, potentially affecting the ability of wetlands to perform these key services (Brooks et al., 2012). For instance, studies report decreases in the duration of snow cover and a reduction in snowpack water content, concurrent with observed increases in air temperatures (Rangawala et al., 2012), which could potentially create periods of drought or low flow in mountain wetlands. Moreover, earlier extreme rain events during spring may quicken snowmelt, leading to the rapid onset of flood events (e.g. Pomeroy et al., 2016). These facts, coupled with the ecological importance of wetland in intermountain regions, provides the motivation to better understand how hydroclimate processes effect wetland functions.

The leeward slopes of the Canadian Rocky Mountains support an abundance of wetland ecosystems, making them an excellent location to study hydrological processes. Stable water isotopes of hydrogen and oxygen (δ^2H and δ^{18}O), and Deuterium Excess (d-excess), in combination with climate data, provide a useful and increasingly applied method for integrating hydrological process information, and can be used to identify spatiotemporal patterns (McDonnell and Bevan, 2014). D-excess in precipitation, defined by Dansgaard (1964), is mainly related to climatic conditions (temperature, relative humidity, and wind speed) at moisture source regions and is widely used to trace moisture sources and recycling (Cui et al., 2017). Moisture evaporated from land surface is formed by plant transpiration and evaporation of water from soils and lakes (Froehlich et al., 2008). The latter component is high in d-excess because of kinetic isotope fractionation during evaporation. Recycling of such moisture to the atmosphere increases the d-excess of the atmospheric vapor and consequently of the precipitation formed by condensation of this vapor. Thus, the systematic differences in d-excess signals in

various water sources/types within watersheds generally reflect the significance of evaporation loss in the water balance of hydrological components (Whitfield et al., 2010).

Craig (1961) established that seasonal and climatically driven interactions between the δ^2H and $\delta^{18}O$ content of water in precipitation results in a Local Meteoric Water Line (LMWL), which can be linked to water sources to assess the relative importance of seasonal precipitation contribution to regional surface waters (Wassenaar et al., 2011). Linear deviations from the LMWL, referred to as the Local Evaporation Line (LEL), are a result of evaporation of surface water that enriches the heavy oxygen and hydrogen content of remaining water (Craig and Gordon, 1965). The LEL can be used to provide basin-scale estimates of the degree of evapotranspiration (ET) and water inflow to individual water bodies (Gat, 1996; Wassenaar et al., 2011). The slope of the LEL reflects the influence of varying local conditions (temperature, relative humidity, wind speed, etc.) naturally integrated over the evaporative season (Gibson et al., 1993). Relative displacement along the LEL for a given evaporation rate is also characteristic of local conditions, as is the limiting enrichment (Gibson et al., 1993). The application of stable isotope end-members, in combination with climate data, will contribute to the understanding of the hydrologic processes that support wetlands, and provide insights into the implications of continued environmental change (Penna et al., 2014).

Water resources of the Canadian Rocky Mountains, often referred to as the "water tower" of Canada, are highly important for drinking water, agricultural uses, and natural habitat (Hrach, 2021; Morrison et al., 2015). Estimations of how hydroclimatic variations will impact wetland source water trends in the south-eastern Canadian Rocky Mountains are important however, few studies have addressed this because of the physical challenges presented by rugged landscapes and remote location. Combining new and historical datasets, this study seeks to investigate spatiotemporal patterns in wetland source waters using stable isotopes of hydrogen and oxygen (δ^2H and $\delta^{18}O$), and assess relevant hydrometric controls throughout the Kananaskis Valley, Alberta, Canada. The objectives of this paper are to: I) understand the influence of evaporative fluxes on extensive wetland sites across an elevation range, and II) determine the spatial and temporal variability in intensive wetland source waters (e.g. groundwater, rain, snow, stream, and surface water) over multiple seasons, and the factors influencing them (e.g. climate controls and elevation) in the Kananaskis Valley.

3.2 Materials and Methods

3.2.1 *Study Area*

Data for this research was collected throughout a ~1981 km^2 area in the eastern region of the Canadian Rockies, all located within 50 km of Calgary, Alberta. Sites were located in the Kananaskis River Valley (50 46'43.14" N, 115 20'32.89" W), part of the Stoney-Nakoda First Nations reserve, and three municipal districts. The study area ranges in elevation from 1280 to 1980 m a.s.l., with the highest elevation wetlands located in Peter Lougheed Provincial Park (Figure 3-1). The study area forms the western margin of the Western Canada sedimentary basin and is therefore geologically complex (Morrison et al., 2015). Strata (sandstone, limestone, shale, and dolomite) are folded and faulted, ranging in age from Cambrian to Cretaceous (Toop and de la Cruz, 2002), and are covered by glacial, lacustrine, and fluvial materials (Gignac et al., 1991). The mountain region is characterized by glaciated U-shaped valleys, with moraines at higher elevations and valleys dissected by rivers at lower elevations. Land use activities in the area are restricted with uses such as forest harvesting permitted in the Improvement Districts but not in Provincial Parks. Land use in alpine regions includes recreational hiking, camping, and skiing, while lower elevation regions are characterized by a rolling topography and more varied uses, such as recreational vehicles and equestrian activity.

The climate of the Kananaskis Valley is subject to spatiotemporal variation due to orographic influence. Precipitation follows a continental pattern and is heaviest in July. It varies from 400 to 550 mm annually, with potential evapotranspiration in the same range, making the area semi-arid (Toop and de la Cruz, 2002). The closest Environment and Climate Change Canada (ECCC) weather station (ID 3053600) with 30+ years of climate records is located in the north-eastern margin of the study area (51.01 N, 115.03 W) at an elevation of 1,391 m a.s.l. The warmest month, July, is 14.1°C on average, while the coldest month, January has a mean temperature of -7.5°C. Although, temperatures are quite variable with extremes of 33.9°C and -45.6°C (Figure 3-2). Weather changes are largely controlled by disturbances in the circumpolar westerlies that allow for continuous movement of airmasses through the region (Harder, 2008). During the winter months, climate is controlled by two major airmasses: the Pacific airmass and Arctic airmass that develop over Siberia and the Arctic Ocean, respectively. In the Kananaskis region, Chinook winds commonly occur during winter months and can affect the local climate and hydrology because of their warm and dry conditions (Harder, 2008). During the early summer months, the Kananaskis

Valley receives limited sunlight as a result of low temperatures that bring cloudy, moist air to the region. During the summer months, Chinook winds create low nighttime relative humidity that is largely independent of vegetation cover, site, and topography (Whitfield et al., 2014). At higher elevations in the valley, the majority of annual precipitation occurs as snow or a mixture of rain and snow with the greatest snow depths in the upper bands of elevation.

3.2.2 Wetland Identification
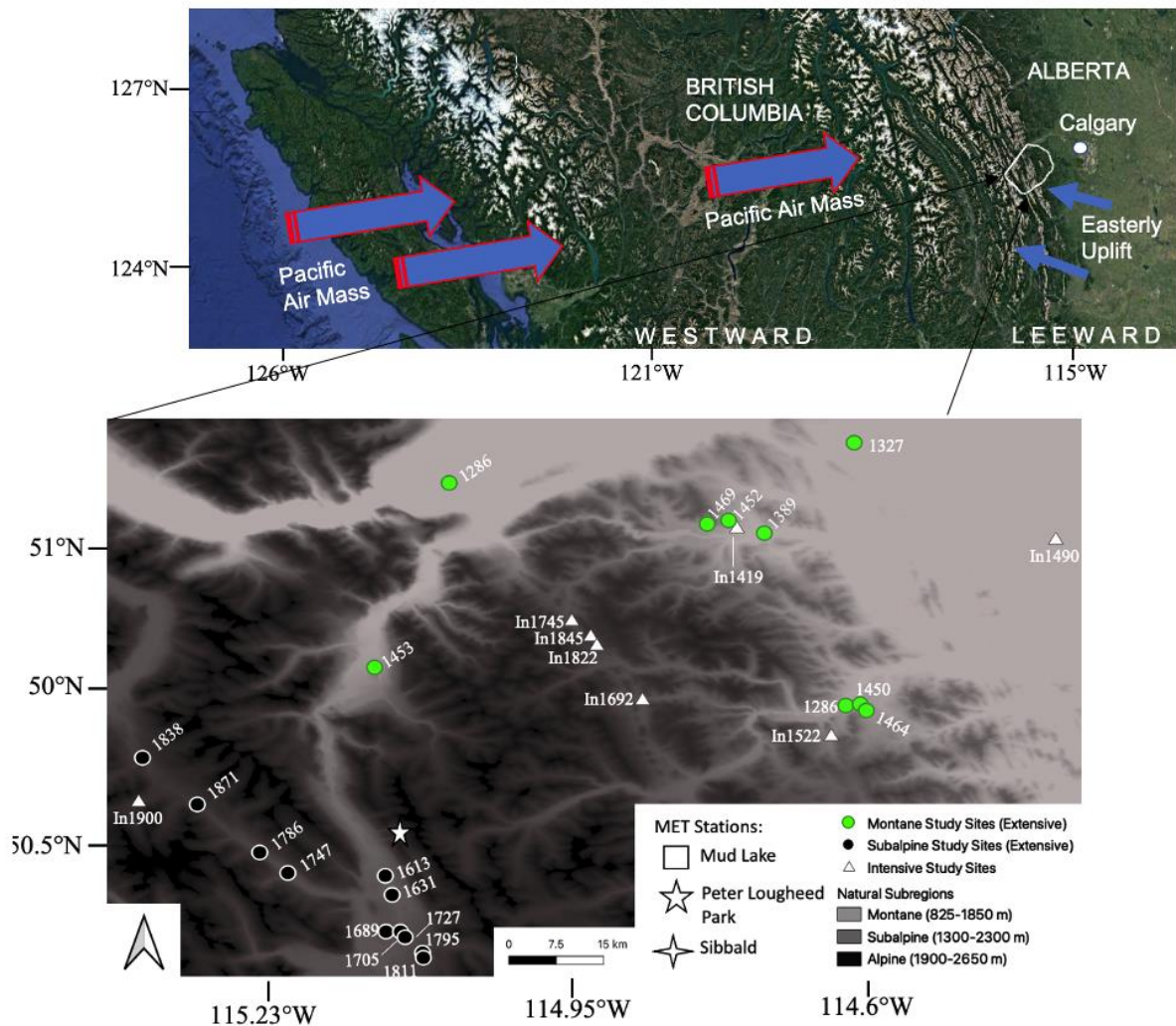
Figure 3-1. Digital Elevation Map of study site using geospatial data from Government of Canada. Natural Subregions of Interest are depicted by color. Extensive sites in the Montane Natural Subregion are shown in green circles (n= 9) and sites in the Subalpine Natural Subregion are shown by black circles (n=11) with white outline. Intensive sites are depicted by white triangles (n=8). Top imagine is ap of surrounding area including influential air masses from the Pacific Ocean and Easterlies from the Gulf of Mexico. Study site is shown by white circle. Classic orographic effects occur on the westward side resulting in rain out of heavier isotopes at low elevations (shown). Mixing of pacific air mass and easterlies occur on the leeward side.

Eight intensive wetlands, at different elevations, were studied during the 2018, 2019, and 2020 growing seasons. Intensive wetlands were established in 2018 and were equipped with a groundwater monitoring well and precipitation bucket to collect groundwater and rain water samples for isotopic analysis. The number associated with each identifier is the elevation in m a.s.l. of that specific site. In 2012, 529 wetland sites were established by Morrison et al. (2015) to assess beaver habitat. Original inventorying of extensive wetlands involved general analysis of aerial imagery in 2007 and 2008. The distinction between peatland and mineral wetlands was based on soil organic matter content by mass, where peat has >30% organic matter content and >17% organic carbon content (Soil Classification Working Group, 1998). Samples of the top 40 cm from the core were sealed in polypropylene bags and then burned in a muffle furnace at 500 °C to determine percentage of organic matter. In 2012, a subset of 90 wetland sites from the original 529 sites were selected for isotopic sampling of beaver pond water, no other wetland source waters were sampled at extensive sites. For the purpose of this study, a smaller subset of 20 sites (extensive) were randomly selected from the previous 90 sites, then divided into their Natural Subregions; Upper Foothills, Montane, or Subalpine as shown in Figure 3-1. The sampled wetlands' elevation ranged from 1286 m a.s.l. to 1971 m a.s.l., intersecting the elevation ranges of Upper Foothills, Montane, and Subalpine Natural Subregions; 950 – 1750 m a.s.l., 825 – 1850 m a.s.l., and 1300 – 2300 m a.s.l., respectively (Downing and Pettapiece, 2006). From this point forward, the Upper Foothills and Montane were grouped and referred to as the Montane Natural Subregion since both Natural Subregions are directly below the Subalpine Natural Subregion depending on their location in respect to the Bow River (Reynolds, 2020).

The Montane Natural Subregion covers 1.3% of the province that ranges in elevation from 825 – 1850 m a.s.l. (Downing and Pettapiece, 2006). The temperatures range from -10.0 °C and 13.9 °C and has 589 mm of mean annual precipitation (Downing and Pettapiece, 2006). The habitat contains grasslands and mixed or aspen (*Populus* species), lodgepole pine (*Pinus Contorta*), Douglas fir (*Pseudotsuga menziesii*), and white spruce forests (*Picea glauca*) (Downing and Pettapiece, 2006).

The Subalpine Natural Subregion covers 3.8% of the province that ranges in elevation from 1300 – 2300 m a.s.l. (Downing and Pettapiece, 2006). In the Upper Bow River Basin, this Natural Subregion occurs above the Montane or Foothills Natural Subregion depending on the location (Downing and Pettapiece, 2006). North of the Bow River, the Subalpine is above the Upper

Foothills Natural Subregion and south of the Bow River, the Subalpine is above the Montane Natural Subregion. In this study, no sites intercept with the Foothills Natural Subregion. The temperature ranges from -11.7 °C and 11.3 °C and has 755 mm of mean annual precipitation (Downing and Pettapiece, 2006). The habitat contains mixed conifer forests of lodgepole pine (*Pinus Contorta)* and Engelmann spruce (*Picea engelmannii*) (Downing and Pettapiece, 2006).

3.2.3 *Isotope Data Collection*

Surface water samples from beaver ponds at extensive sites (n=20) were collected in 2012 during the pre- and peak- growing season (June-July) by Morrison et al. (2015), and again in August-September of 2020. Samples were collected in ponds with low water movement. Surface sample collection at intensive sites (n=8) occurred during 2018 and 2019 throughout the growing season at sites with sufficient standing water. Intensive sites were then sampled again during September of 2020. Detailed collection methods are described in Chapter 2. In brief, water samples were bottled with minimal headspace and stored at room temperature (never refrigerated or frozen to limit phase changing) before processing. The temporal record, and number of samples collected at each site, is summarized in Table 3-1.

Groundwater was sampled from a repeat well location during the snowmelt period starting in May, through the late growing season period in September at intensive sites in 2019. The groundwater table was consistently at the surface during the pre and peak growing seasons. However, the water table fell below the well depth (1 m) during the end of the peak- growing season and into the post growing season at several of the intensive sites.

Rain sample collection began at the end of the peak- growing season in 2018 at intensive sites when collectors were installed. In 2019, rain was measured monthly throughout the growing season (May-September) when there were precipitation events. Rain collectors were only available at two sites (In1900 and In1419) during the 2020 sampling campaign. Rain collectors were built to limit evaporation of samples between sampling periods. A plastic hose was sealed watertight to the bottom of a funnel, which was then sealed to the top of a water reservoir container. The hose was cut with enough length to coil on the bottom of the reservoir to ensure the water level of the collected samples topped over the hose, limiting evaporation and phase change of the sample. A Ping-Pong ball was placed in the top of the funnel to limit evaporation further.

Snow samples were only collected for pre- and post- growing season sampling periods due to availability during 2018 and 2019. Snow was collected any time it was present, which was usually in spring during snowmelt or fall when accumulation was starting. Samples were collected using a plastic bag, which were left to melt at room temperature to ensure complete mixing and no phase change before being sub-sampled into 20 mL poly-seal sampling bottles. The snow was never deep enough to take snow cores so this method was not used.

Stream samples were collected throughout the 2018 and 2019 growing seasons (May-September) at intensive sites with flowing streams. All 2020 stream samples were collected late in the growing season again due to restricted access to sampling sites. Samples were taken by dipping uncapped poly-seal sampling bottles into streams facing against the current to ensure minimal contact with water sample. Samples were immediately sealed to minimize evaporation.

All water samples collected in 2018, 2019, and 2020 were analyzed at the Environmental Isotope Laboratory (EIL) at the University of Waterloo, Waterloo, Ontario. Samples were processed with the $\delta^{18}O$ and δ^2H LGR-OA-ICOS Laser System using methods as described by the EIL, University of Waterloo (LGR, 2010; Berman et al, 2013). Quality control was maintained by running a range of water standards including VSMOW (Vienna Standard Mean Ocean Water) and VSLAP (Vienna Standard Light Antarctic Precipitation) from the International Atomic Energy Agency (IAEA). Duplicates were run at a minimum of every fifth samples. Each run also included an in-house check standard for QA/QC of each individual sample batch. Electric conductivity was assumed to be in normal range due to past measurements in the area. Samples collected in 2012 were analyzed at the McDonnell Hillslope Hydrology Lab at the University of Saskatchewan using the same equipment and methods described above.

3.2.4 Meteorological Data

Meteorological (MET) data, including temperature and precipitation, were used from 3 separate stations each shown in Figure 3-1. Mud Lake data was collected by instrumentation on a tripod positioned 4.15 m above the ground near site In1900. MET data included relative humidity and temperature measured with a HMP 155 (Viasala, Finland), as well as rainfall. Rain precipitation was measured at Mud Lake at 2.03 m above ground using an Ott Pluvio 400 (Ott Hydromet, CO, USA). The Peter Lougheed Park station is located at 1622 m a.s.l. and is operated by Alberta Sustainable Resource Development. The Sibbald meteorological station is positioned at 1490 m

a.s.l. and is equipped with a Rotronic HC2-S3 probe to measure air temperature and a Texas Electronics TE525 tipping bucket to measure rainfall. The MET station is part of the Canadian Rockies Hydrological Observatory.
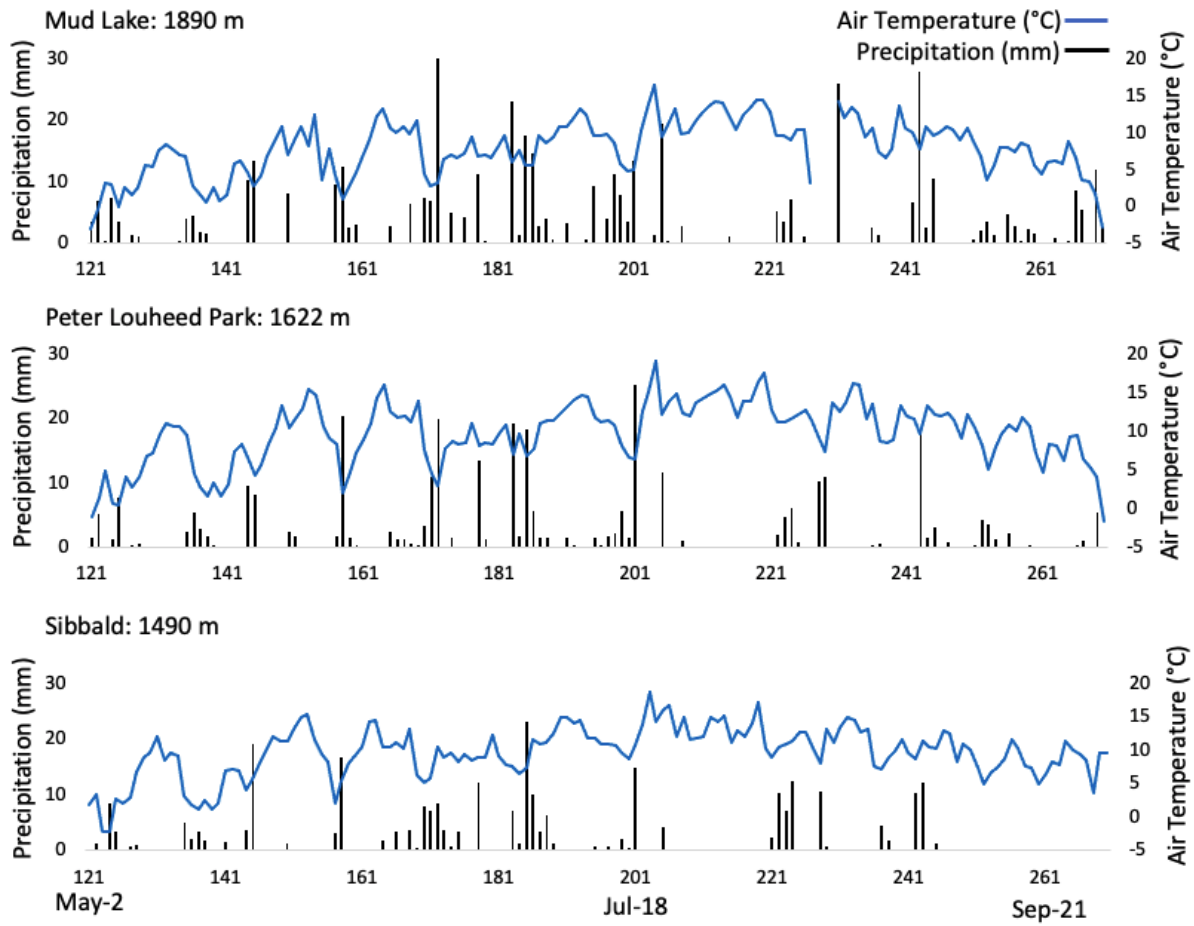
Figure. 3-2. Basic meteorological conditions including precipitation and air temperature from Mud Lake, Peter Lougheed Park, and Sibbald. Shown are the 2019 daily averages from May 1st – September 30th.

3.2.5 Data Analysis

D-excess was calculated as $\delta D = \delta^2 H - 8* \delta^{18}O$ (Dansgaard, 1964). D-excess is associated with kinetic fractionation, which is typically indicative of evaporation or condensation (Ala-aho et al., 2018). When d-excess values equal 10, the sample is located on the Global Meteoric Water Line (GMWL). Samples with values <10 plot below the GMWL and signal a deviation from equilibrium fractionation conditions, indicating the samples were subject to evaporative influence. In addition, because of the close relationship between $\delta^{18}O$ and δD in precipitation, values can reflect different environmental characteristics in precipitation moisture sources. Thus, d-excess was used in this study to interpret evaporative and non-evaporative signals across the

39

landscape, and identify meteorological factors associated with different moistures sources throughout the growing season.

Volume weighted means were calculated for rain and d-excess for the 2018 and 2019 growing seasons using, where δ_i is the measured isotopic value during the precipitation event and P_i is precipitation (mm) during that period (Lee et al., 2003). Rain samples were collected monthly from intensive sites for isotopic analysis, and precipitation data was used from Mud Lake and Kananaskis Valley meteorological stations. Since samples were collected monthly at all sites, values were averaged to get an estimate of rain signals for the region. Precipitation data was totaled for each month to determine the cumulative amount for the collection period.

$$\delta_{WA} = \Sigma(P_i\,\delta_i)/\Sigma P \tag{1}$$

Site	Month	Groundwater			Rain			Snow		Stream			Surface		
		2018	2019	2020	2018	2019	2020	2018	2019	2018	2019	2020	2018	2019	2020
In1419	May	-	1	-	-	-	-	-	-	-	-	-	-	-	-
	June	-	1	-	-	1	-	-	-	-	1	-	-	-	-
	July	1	1	-	-	-	-	-	-	-	-	-	-	-	-
	August	1	1	1	1	1	-	-	-	-	-	-	-	1	-
	Sept.	-	1	1	-	1	-	-	-	-	-	-	-	-	-
	Octobe	1	1	-	1	-	-	1	-	-	-	-	-	-	-
In1490	May	-	1	-	-	-	-	-	-	1	1	-	-	-	-
	June	-	1	-	-	1	-	-	-	-	1	-	-	-	-
	July	-	1	-	-	1	-	-		-	1	-	-	-	-
	August	-	1	-	-	1	-	-	-	-	1	-	-	-	-
	Sept.	-	1	1	-	1	-	-	-	-	1	1	-	-	1
In1522	May	-	1	-	-	-	-	-	-	-	1	-	-	-	-
	June	-	1	-	-	-	-	-	-	1	1	-	1	-	-
	July	1	1	-	-	-	-	-	-	1	1	-	-	-	-
	August	1	1	1	1	-	-	-	-	1	1	1	-	-	1
	Sept.	-	1	1	-	-	-	-	-	-	1	1	-	-	-
	Octobe	1	-	-	1	-	-	1	-	1	-	-	-	-	-
In1692	May	-	-	-	-	-	-	-	-	1	1	-	-	-	-
	June	-	-	-	-	-	-	-	-	-	1	-	-	-	-
	July	1	-	-	-	-	-	-	-	1	1	-	-	-	-
	August	1	-	1	1	-	-	-	-	1	1	1	-	-	-
	Sept.		1	1	-	1	-	-	-	-	1	1	-	1	-
	Octobe	1	-	-	1	-	-	1	-	1	-	-	-	-	-
In1745	May	-	1	-	-	-	-	-	-	-	1	-	1	-	-
	June	-	1	-	-	1	-	-	-	-	3	-	-	-	-
	July	1	1	-	-	1	-	-	-	-	1	-	-	-	-
	August	1	1	1	1	1	-	-	-	1	-	1	-	-	1
	Sept.	-	1	1	-	1	-	-	-	-	-	1	-	-	-
	Octobe	1	-	-	1	-	-	1	-	-	-	-	-	-	-
In1822	May	-	1	-	-	-	-	-	1	1	1	-	-	1	-
	June	-	1	-	-	1	-	-	-	-	1	-	-	-	-
	July	1	1	-	-	1	-	-	-	-	-	-	-	-	-
	August	1	1	1	1	1	-	-	-	1	2	1	-	1	-
	Sept.	-	1	1	-	1	-	-	-	-	-	1	-	-	-
	Octobe	1	-	-	1	-	-	1	-	1	1	-	-	-	-
In1845	May		1	-	-	-	-	-	1	-	-	-	-	-	-
	June	1	1	-	-	1	-	-	-	-	-	-	1	-	-
	July	1	1	-	-	1	-	-	-	-	-	-	1	1	-
	August	-	1	1	-	1	-	-	-	-	1	-	-	-	-
	Sept.	1	1	1	-	1	-	-	-	-	-	-	-	-	-
	Octobe	1	-	-	1	-	-	1	-	-	-	-	-	-	-
In1900	June	-	2	-	-	1	-	1	2	1	2	-	-	-	-
	July	-	-	-	-	-	-	-	-	1	-	-	-	1	-
	August	-	3	19	-	2	-	-	1	1	3	-	-	-	-
	Sept.	-	-	-	-	1	3	-	-	-	2	6	-	-	9
	Octobe	-	-	-	-	-	-	-	-	-	-	-	-	-	-

Table. 3-1. Summary of samples collected from intensive sites from years 2018-2020 throughout the growing season (May-October). The number and type of sample collected at each site during each month is shown.

3.2

Results

3.3.1 Spatial Variability in Isotopes

The spatiotemporal data of Oxygen-18 values in source waters from intensive sites over the 3 growing seasons showed a typical annual cycle (Figure 3-3). Rain samples were isotopically enriched with a median of -17.8‰ and plotted outside the values of groundwater, stream, and surface water. Snow samples were significantly more depleted with a median of -23.5‰ however, they were widely distributed, thus providing a strong tracer for glacial melt versus snowmelt (Figure 3-3). Groundwater, stream, and surface water values were clustered between rain and snow with median values of -19.05‰, -19‰, -19.4‰, respectively. This clustering pattern indicates a degree of infiltration and mixing between surface, stream, and groundwater to a depth of at least 1m where groundwater samples were collected. The LMWL had a slope of 7.48, which is similar to the slope of the GMWL of 8. The slope of the regression line for all water sources was lower than that of the LMWL on the order of 7.2 (snow) > 7.33 (stream), 7
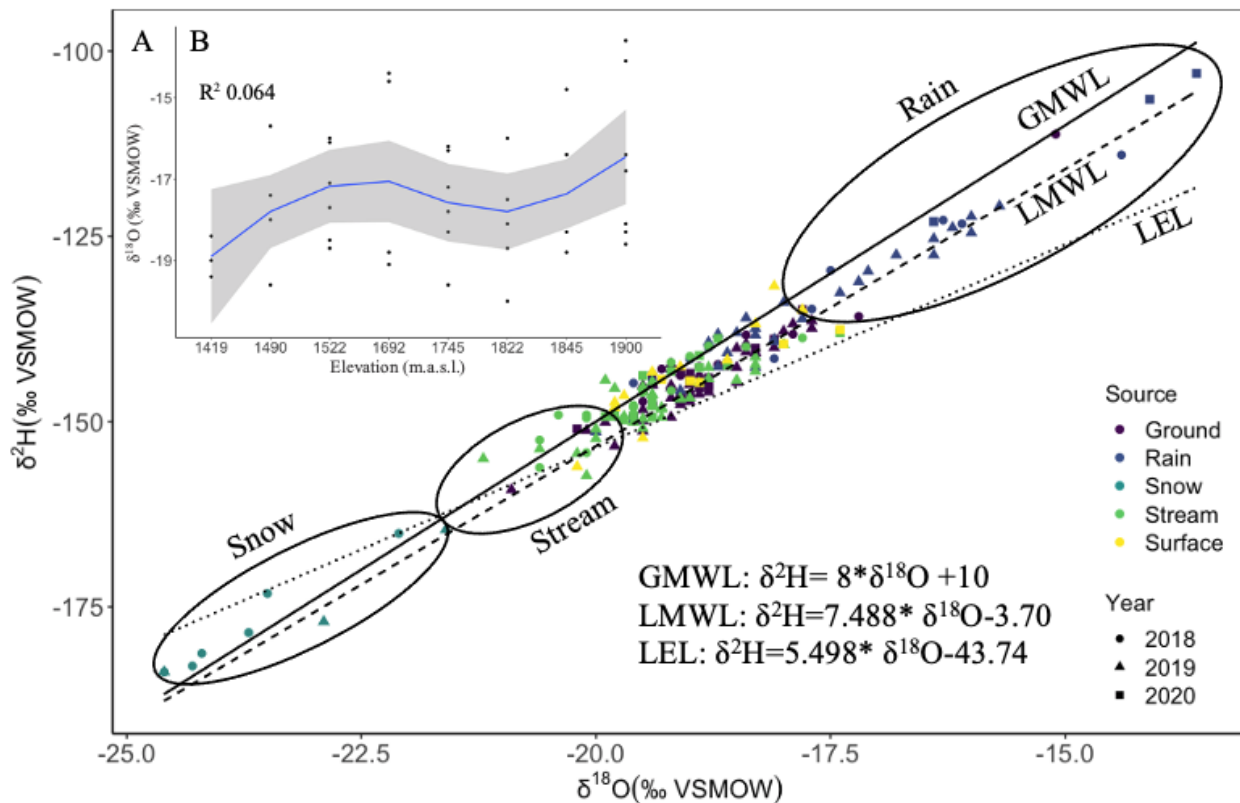
Figure. 3-3. (A) Dual isotope plot, with source depicted by color, of grouped groundwater, rain, snow, stream, surface water samples collected at intensive sites in 2018, 2019, 2020 plotted along the GMWL. LMWL and LEL taken from Katvala et al. (2008) for the Kananaskis Valley, Alberta, Canada. Plot of rain $\delta^{18}O$ vs. elevation (increasing elevation from right to left) shown for all rain data (B).

(groundwater) > 6.7 (surface) > 6.3 (rain), indicating evaporative fractionation for all sources. Surface water values plotted across the GMWL, LMWL, and LEL, which may be associated with contrasting water sources and increased residence times in surface waters versus streams (see source plots, Figure 3-4). Interestingly, rain samples do not show a strong negative linear isotope-altitude relationship. Instead we see a slight depletion in $\delta^{18}O$ near the transition zone between the Subalpine and Montane Subregions before becoming enriched again in the subalpine range. The exact causation of these results is complicated since the precipitation processes on the leeward slopes of the Rockies are heavily influenced by the mixing of air masses and highly variable due to interactions between ambient flow and topography.

The subalpine wetland (In1900) trended more towards the GMWL, despite having a lower slope, indicating greater influence of meteoric water sources (Figure 3-4). Between groundwater, stream, and surface water samples at intensive sites, stream values were the most depleted in $\delta^{18}O$. There is a distinct separation of stream samples (Figure 3-4), originating from both the Montane and Subalpine Subregions during 2018 and 2019. However, the majority
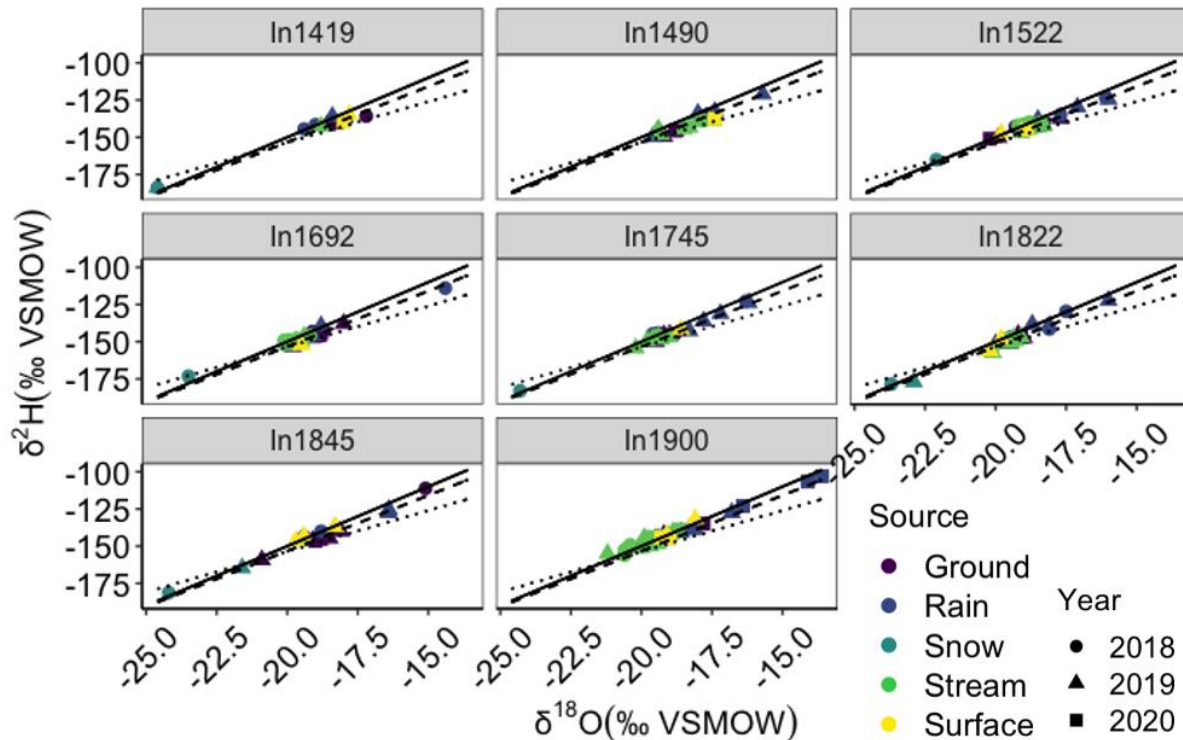
Figure 3-4. Dual Isotope plot grouping all source waters by color and year by shape for all individual intensive sites (n=8). Global Meteoric Water Line (δ^2H - 8* $\delta^{18}O$+10), Local Meteoric Water Line (δ^2H – 7.488* $\delta^{18}O$- 3.7), and Local Evaporation Lines (δ^2H =5.498* $\delta^{18}O$-43.74) are shown as solid, dashed and dotted lines, respectively. The local evaporation lines are for the Kananaskis Valley.

derive from site In1900 and were consistently depleted throughout the growing season, indicating the importance of snow and glacial melt as a component of stream flow generation. Mid-altitude wetlands (1692-1845 m a.s.l.) had the largest distribution of $\delta^{18}O$ values with a minimum of -24.2‰ and maximum of -14.8‰, which is expected for this region (Moran et al., 2007) (Figure 3-4). Observed groundwater, stream, and surface waters values plot close together and remain relatively uniform despite minor fluctuations and slight $\delta^{18}O$ enrichment in subalpine regions (Figure 3-4).

As for $\delta^{18}O$ in wetland pond water at extensive sites, values were overall more widely distributed with a range of -6.5‰ and a median of -18.02‰ (Figure 3-5). Due to partial evaporation from open surface waters, values plotted along the LEL instead of the meteoric water lines, suggesting surface waters were enriched and the evaporated moisture was depleted in the heavy isotopes of Hydrogen and Oxygen (Figure 3-5). Further, d-excess values for all samples plotted below 10‰, the global average d-excess, indicating evaporative influence at all sites (Figure 3-6). The distribution of $\delta^{18}O$ values from the Subalpine Subregion were greater compared to the Montane Subregion however, the Subalpine Subregion average was more
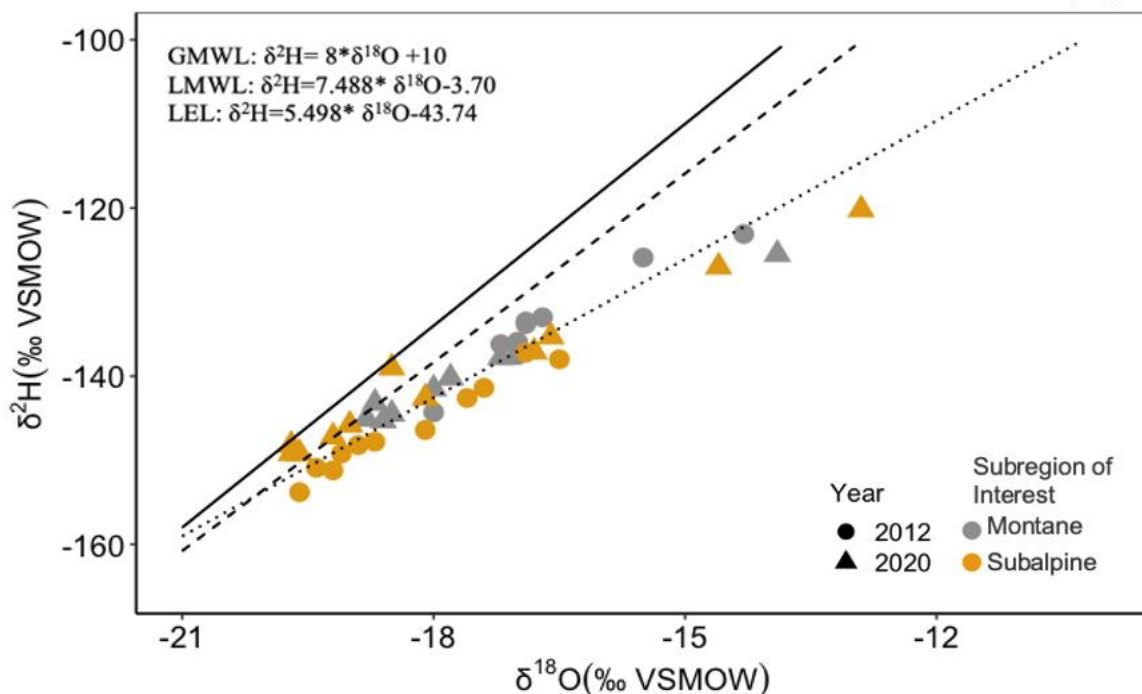
Figure. 3-5. Dual isotope plot of surface water samples collected from beaver ponds at extensive sites during the 2012 growing season (June-July) and 2020 peak- and post-growing season (August-September). Natural Subregion of Interest is depicted by color and year is depicted by shape. LMWL and LEL taken from Katvala et al. (2008) for the Kananaskis Valley.

isotopically depleted (-18 ‰, -17.1 ‰, respectively). Extensive sites did show a stronger altitude-isotope relationship, with values becoming more isotopically depleted (difference of -3‰) as altitude increased, correlated with increasing d-excess for both 2012 (R^2 0.28) and 2020 (R^2 0.11) (Figure 3-6). Correlations between $\delta^{18}O$, d-excess, and elevation were used to test the influence of geographic variables on surface water isotopic values for 2012 and 2020. Significant positive correlations were found between $\delta^{18}O$ values and elevation for 2012 (r=0.47, p<0.01, Figure 3-6). However, despite a slightly stronger altitude-isotope gradient, 2020 data showed a weak, negative correlation that was not significant at p<0.05 (Figure 3-6).
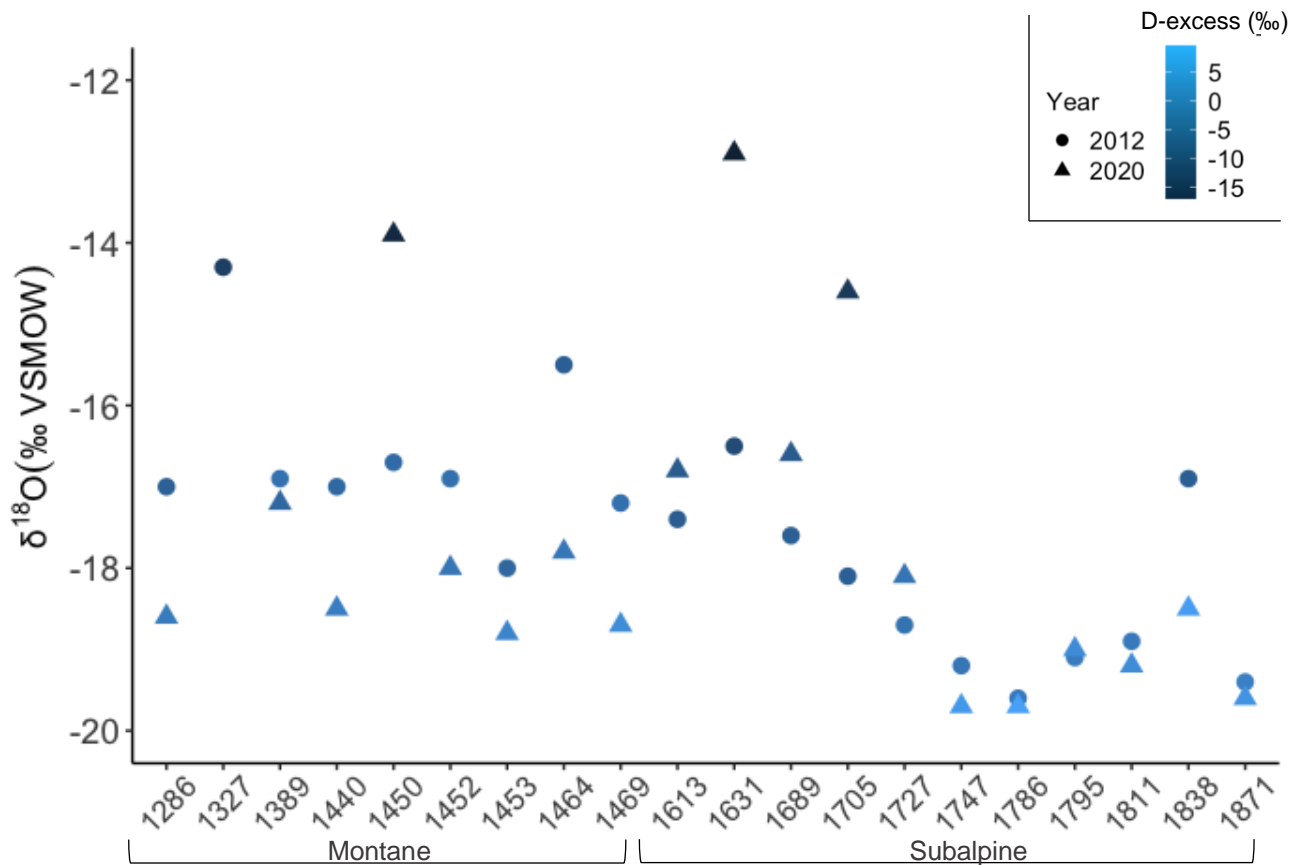
Figure. 3-6. $\delta^{18}O$ and d-excess values shown for extensive wetland pond surface water samples across the Montane and Subalpine Natural Subregions. Year is depicted by symbol, d-excess is depicted by color.

3.3.2 Temporal Variability in Isotopes

Spatiotemporal data for $\delta^{18}O$ values in groundwater, rain, snow, stream, and surface water from intensive sites over the 3 growing seasons are shown in Figure 3-7. Source water data showed a typical annual cycle with depleted winter/spring values and enriched summer values (Figure 3-

7). This annual cycle is best demonstrated during the 2019 growing season due to the completeness of the dataset, in which source waters become more enriched, following seasonal
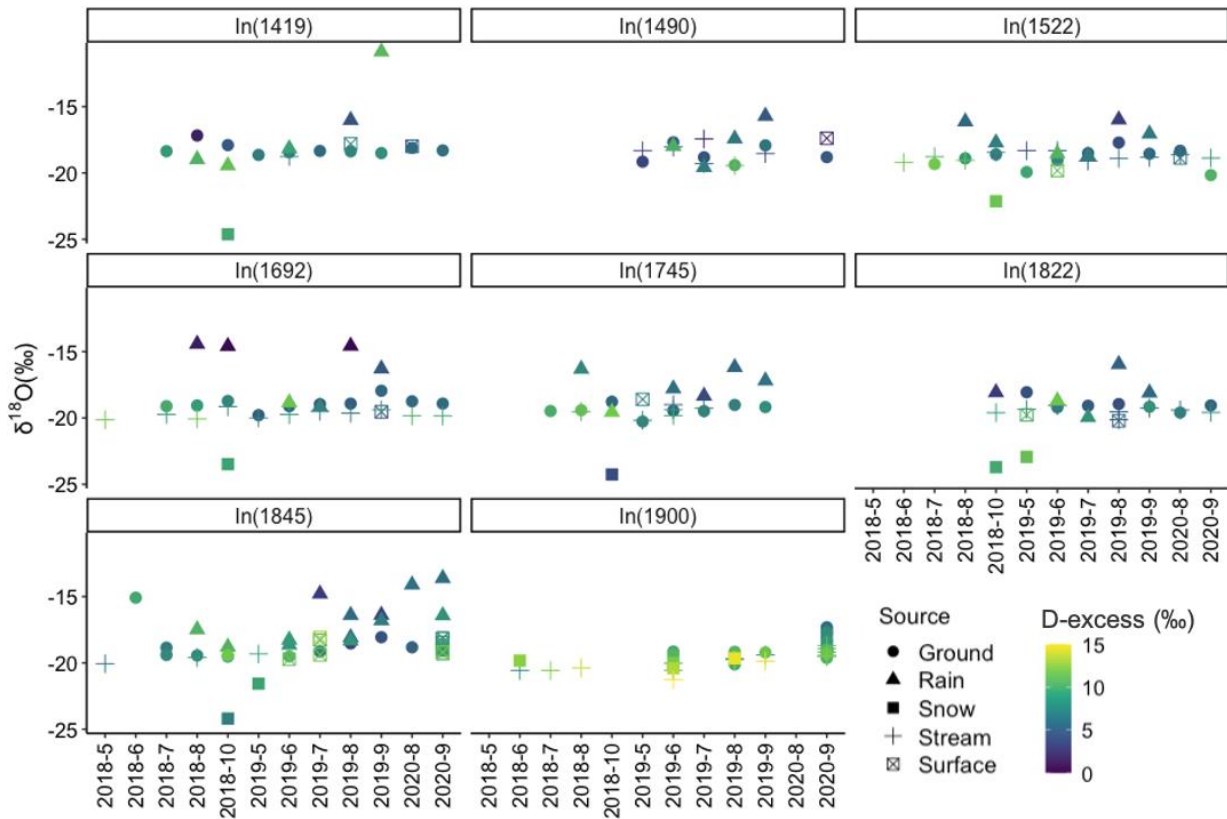
Figure. 3-7. Spatiotemporal plot of $\delta^{18}O$ and d-excess for all intensive sites with precipitation d-excess weighted average shown for 2018 and 2019. D-excess is depicted by color and source waters are distinguished by symbol for groundwater, rain, snow, stream, and surface water.

rain precipitation events (Figure 3-2). Groundwater showed the highest temporal variability followed by surface water and streams. Interestingly, stream water was consistently more depleted than groundwater at all sites (Figure 3-7). Within site In1900, the distribution of $\delta^{18}O$ groundwater signals was much greater at the end of the growing season relative to lower elevation sites, which could be caused by inputs from different water sources (e.g. glacial melt, upslope runoff).

D-excess was used in this study to assess evaporation effects in the landscape and identify moisture sources for precipitation. Results show strong seasonality with high d-excess values occurring during the peak-post growing seasons and low values during pre-growing season (Figure 3-7). Not surprisingly, d-excess did not show strong seasonality within individual sites, but did increase with rising elevation (Figure 3-7). Site In1900 had the highest d-excess

values, with 2 source averages plotting above the global average (stream (10.1 ‰), and snow (13.5 ‰)) (Figure 3-7). This site experiences minimal evaporative influence, indicating that the enriched δ^{18}O values are potentially a result of environmental characteristics and not evaporative fractionation. The volume weighted average of precipitation d-excess calculated from intensive data for the study region is 7.27 % (2019) and 8.34 % (2018), which is below the average d-excess of the global meteoric water (Figure 3-8). In general, the median d-excess value of snow was the highest (11.21, 8.34 ‰), followed by stream (9.51, 7.25 ‰), surface (NA, 9.49 ‰), and groundwater (8.60, 6.87 ‰) for 2018 and 2019, respectively. Most importantly, the median d-excess of groundwater plotted below the median of precipitation d-excess in 2019 during pre-, peak-, and post growing seasons, indicating continued evaporative influence throughout the growing season. Although the d-excess median of groundwater plotted above the median of precipitation d-excess in 2018, there were values that plotted below 7.27 ‰ however, these derived from Montane sites primarily during the peak-post growing season (Figure 3-7).

The distribution of δ^{18}O data from surface waters at extensive sites showed progressively more variation throughout the growing season, especially from the Subalpine Subregion, and depleted average δ^{18}O values for the snowmelt period that remained relatively depleted through
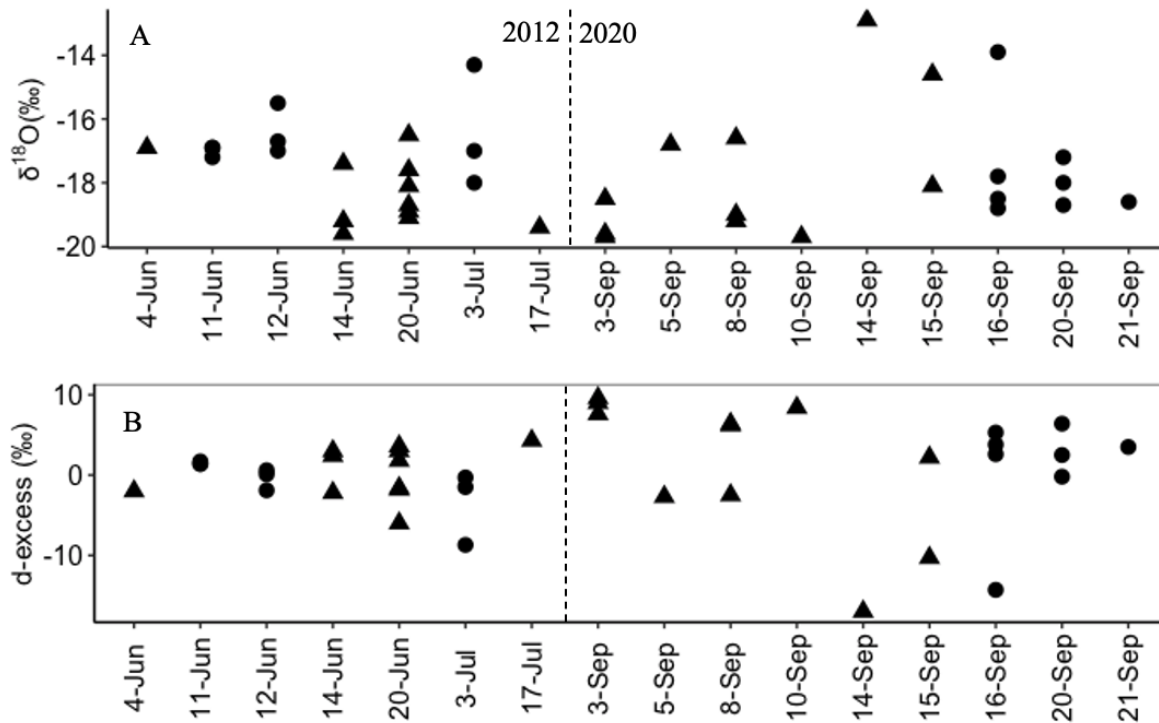
Figure. 3-8. Time-series distribution of δ^{18}O (A) and d-excess (B) values from extensive sites for each sampling period in 2012 and 2020. Natural Subregions are depicted by shape for clarity. The Montane Natural Subregion is represented by circles and the Subalpine Natural Subregion is represented by triangles.

the peak 2012 growing season (Figure 3-8). The δ^{18}O composition of surface water from Montane sites showed relatively damped variability, which could be due to the gap in data between the pre- and post- growing seasons. We would expect enrichment of δ^{18}O during the peak- growing season correlated with increased temperatures and precipitation. The average δ^{18}O during the pre-peak growing seasons was -17.41 ‰ ($\pm$1.17) and post growing season was -17.5 ‰ ($\pm$1.6). In 2020, samples were collected during the post- growing season generally appeared to be more depleted in δ^{18}O except at subalpine sites, where δ^{18}O values remain between -18.5‰ and -19.5‰, indicating mixed moisture sources and precipitation inputs (Figure 3-8).

3.2   Discussion

Mountain wetland ecosystems are expected to be among the most sensitive to changing climate as their persistence depends on factors directly influenced by climate (e.g. precipitation, snowpack, evaporation). Despite their importance and sensitivity, such processes tend to be understudied due to the difficulty of data collection in rugged mountain landscapes. This research addressed the hydroclimate processes that control wetland function, and how they affect wetland source water composition across spatiotemporal scales. The objectives of this paper are to: I) understand the influence of evaporative fluxes on extensive wetland sites across an elevation range, and II) determine the spatial and temporal variability in intensive wetland source waters (e.g. groundwater, rain, snow, stream, and surface water) over multiple seasons, and the factors influencing them (e.g. climate controls and elevation) in the Kananaskis Valley. We used stable water isotopes and climate data to investigate objectives I and II. This research is important because climate patterns in montane regions are changing, and it is currently not clear how hydroclimate controls will effect wetland dynamics. Overall, evaporative fluxes from wetland source waters followed the expected seasonal trend, exhibiting stronger evaporative signals during the summer associated with high temperatures and longer sun exposure. Consistent with results from Chapter 2, isotopic signals indicate mixing between source waters within individual wetlands, demonstrating water derivation from both rain and snow.

3.2.1   *Spatial Variability In Isotopes*
Plotted groundwater, rain, snow, stream, and surface water data from intensive sites showed a normal δ^{18}O distribution, with enriched rain and depleted snow signatures, consistent with global

patterns (Ala-aho et al., 2018; Taziolo et al., 2019; Shi et al., 2019). Minimal variability of isotopes in groundwater, stream, and surface waters, compared to rain and snow indicates mixing of snowmelt/rainfall throughout the growing season with stored water in the landscape. Comparing the hydrogen and oxygen isotopes of groundwater and stream water with the LMWL, it can be seen that points of stream water and groundwater are located at the upper left of the LMWL, and are close to the atmospheric precipitation line. This indicates that precipitation has a replenishing effect on stream water and groundwater, especially during the late summer. This pattern is consistent with results from a similar study, in which connections between source waters and streamflow generation were assessed in a comparable mountain setting (Leuthold et al., 2020; Shi et al., 2020). The observed increase in d-excess and δ^{18}O depletion in high elevation streams (1800-1900 m a.s.l.), was also reported in Leuthold et al. (2020), and is likely the result of substantially more snow than rain precipitation and the effects of cool, short summers on meteorological conditions (Theriault et al., 2018). The more enriched δ^{18}O median in streams (-18.8 ‰) and groundwater (-18.5 ‰) at low elevations could indicate preferential sourcing of stream water from isotopically heavier rain, longer groundwater residence times allowing for rain infiltration from the surface, and/or water enriched by evaporation from storage in wetland landscape (Ala-aho et al., 2018). The overall more enriched δ^{18}O median of groundwater (-19.00 ‰) compared to streams (-19.75 ‰) is the result of evaporative influence confirmed by significantly higher d-excess in streams (10.55 ‰), as compared to groundwater (6.5 ‰).

The observed ambiguous δ^{18}O-elevation gradient of rain is likely due to temporally complex, local climate conditions on the leeward side of the Canadian Rocky Mountains (Figure 3-3). In lee-slope environments, the δ^{18}O-elevation relationship often reflects the patterns of moisture transport and deposition, and is significantly altered by processes such as sub-cloud evaporation and mixing of different air masses (Kong and Pang, 2016; Moran et al., 2007). Under specific circumstances such processes can create an ambiguous or inverse δ^{18}O-elevation relationship, whereby δ^{18}O becomes more enriched with increasing elevation. In a meta-analysis by Poage and Chamberlain (2001) of observed δ^{18}O-elevation gradients from 68 different studies worldwide, all but two studies reported δ^{18}O depletion with altitude, one of which was within the eastern Canadian Rocky Mountains. Kong and Pang (2016) reported similar findings as a result of inverse orographic effects, at a comparable latitude (46° N) and elevation range, in a semi-arid alpine setting in the Tianshan Mountains of Northwest China. In the Canadian Rocky Mountains,

inverse δ^{18}O-elevation gradients specifically occur when easterly systems from the Gulf of Mexico bring rainfall from continued rainout of air masses as they span topographic barriers (Figure 3-2) (Theriault et al., 2018). Then, continued Rayleigh fractionation distillation (removal of δ^{18}O from cloud) occurs as systems are pushed upwards, which creates a reverse orographic effect (Moran et al., 2007). Since the results from this study do not show a strong linear δ^{18}O-elevation relationship (R^2 0.0076), there is likely mixing of Pacific air masses and continental weather originating from the southeast, creating such ambivalent results (Smith, 2008).

Surface waters in mountain landscapes are subject to a variety of environmental factors that influence their isotopic composition (Kendall and Coplen, 2001). The specific focus on wetland ponds (extensive sites) in this study is unique and provides an opportunity to evaluate hydrometeorological influence and hydrologic connectivity in wetland abundant landscapes. The range of isotopic signatures of subalpine wetlands was greater than those of the Montane Subregion likely due to the overlap in Natural Subregion elevation ranges, and therefore characteristics of subalpine versus montane wetlands. For example, a greater presence of open grasslands in the Montane Subregion promotes evaporation from surface waters driving more enriched δ^{18}O signals. This is evident in Figure 3-5 as the majority of data from Montane sites trend along the LEL. The higher end of the subalpine range is dominated by forested landscapes and more commonly exhibits complex terrain, interfering with sunlight. Our results demonstrate this effect as d-excess drops off at higher elevations. Shade effects are clearly shown in Hrach et al. (2021) in which a shaded subalpine wetland received significantly less sunlight throughout the growing season compared to an unobstructed site.

3.2.2 *Temporal Variability In Isotopes*

Temporal analysis of stable water isotope data from intensive sites aligns with studies that seek to map patterns of δ^{18}O and d-excess in wetlands, however, they are located primarily in low-elevation environments, or investigate large lake and river systems (Ala-aho et al., 2018; Carol at al., 2020; Brooks et al., 2018). Similar to temporal patterns described by Ala-aho et al. (2018) in a low elevation, cold region climate, all sites showed suppressed variability of source water signals within individual sites, but slight enrichment from the pre- to post- growing season. δ^{18}O in streams was slightly more depleted during snowmelt (May) (-19.99 ‰ ±0.6) than the peak- growing season (July & August) (-19.35‰ ±0.7). There was not steady linear enrichment of δ^{18}O throughout the peak- and post- seasons, providing evidence of a longer snowmelt period, close proximity to

depleted groundwater reserves, and/or minimal evaporative influence (Figure 3-7). The general seasonal similarities between $\delta^{18}O$ content of streams and groundwater, which is documented in wetlands, shows that groundwater that supports wetland function is supplied by inflows from stream water as well as from rainfall (Carol et al., 2020). Observed $\delta^{18}O$ enrichment of stream water during the peak- and post- growing seasons could be explained by evaporative fractionation as shown by decreasing d-excess values, increased rainfall inputs, or greater mixing due to reliance on groundwater for stream flow generation.

The overall temporal isotopic analysis of $\delta^{18}O$ and d-excess in wetland surface waters at extensive sites were highly variable, and the exact causation is difficult to discern. During the 2012 pre- growing season, both Montane and Subalpine sites follow an expected distribution with $\delta^{18}O$ values decreasing from June to July. The temperature profiles from the subalpine versus montane field site are similar during this period however, fluctuations throughout the growing season are not as severe at the Montane site, and temperatures are overall more mild. These conditions could explain the more depleted $\delta^{18}O$ signatures from the Montane sites. During late June and into early July, surface waters became significantly more depleted in $\delta^{18}O$ coupled with increased d-excess, especially at high elevations. This is likely the result of a later and prolonged snowmelt at sites in the Subalpine region and a combination of higher temperatures and rainfall in the Montane region. During the peak growing season, the damped variation in d-excess is likely from persistent inputs of snowmelt and rain water, minimizing evaporation from surface waters. Similar studies documented $\delta^{18}O$ enrichment in surface waters in alpine and subalpine regions during the peak-growing season, coupled with decreased d-excess values, indicating that the distribution of samples along the LEL are likely the result of a combined precipitation inputs and evaporative effects due to prolonged residence times (Shi et al., 2019; Hayashi et al., 2004). Moreover, d-excess values of stream and groundwater from intensive sites have a higher average than surface waters throughout the growing season, again indicating poor connectivity between wetlands, and minimal mixing between surface waters and other water inputs. A possible explanation for stunted hydrologic connectivity is the documented effects of beaver populations on hydrologic flow paths. Beaver damns are known to temporally change water storage and connectivity in the eastern Canadian Rocky Mountains (Ronnquist and Westbrook, 2021). However, this requires further research to determine the extent of beaver influence.

3.3   Conclusions

This study aims to investigate spatiotemporal patterns of hydrogen and oxygen (δ^2H and δ^{18}O) in wetland source waters, and assess relevant hydrometric controls throughout the Kananaskis Valley, Alberta, Canada. The extensive spatiotemporal scale of stable water isotope sampling throughout the Kananaskis Valley allowed for an improved conceptual understanding of surface water residence times and dominant runoff generation processes in this wetland-influenced landscape. Our findings suggest significant surface water storage capacity is involved in intensive isotopic mixing of snowmelt and that relatively small proportion of water released from snowmelt infiltrates to groundwater during the pre- growing season. The evaporation fluxes from extensive sites decreased with increasing elevation (high d-excess value), and isotopic values become further removed from meteoric water lines. Based on this, we hypothesize that the primary runoff generation mechanism changes throughout the growing season. Snowmelt water is readily mobilized to streams during the pre- growing season, but during the peak- growing season water already stored in wetlands is displaced and maintains hydrologic connectivity between mountain streams. For these wetlands, a change in the water balance in favor of enhanced evaporation (due to warmer and longer summer season than present) will not only lead to greater water loss from the wetlands themselves, but may also reduce the water inputs from their catchments. As indicated by the variations in isotopic signatures from wetlands in the Montane versus Subalpine regions, individual ecosystems will be adversely affected. Earlier spring snowmelt and melting of glacial ice in future years may eventually lower the water table, which is unfavorable to most existing wetlands, and in extreme scenarios, may result in drying of wetlands in the Montane and Foothills Natural Subregions (Woo et al., 2006).

The improved conceptual understanding of evaporative fluxes and runoff generation gained in this work is important framework that can be tested with modelling and provide insights relevant to future response of wetland ecosystems to changing hydrological processes in the Canadian Rocky Mountains.

Chapter 4: Thesis Summary and Limitations

4.1 Summary

It is well known that the Subalpine and Montane Subregions of the Eastern Canadian Rocky Mountains will undergo changes in hydrometeorological processes as a result of anthropogenic climate change (Adhikari and Marshall, 2013; Fyfe and Flato, 1999). Current reports highlight that snowpack reduction, earlier spring snowmelt, and changing vegetation dynamics in high elevation regions are associated with warmer air temperatures and overall greater water loss throughout the growing season (Tague and Dugger, 2010). In such environments, wetlands are crucial hydrologic components that rely on source waters (e.g. snowmelt, groundwater discharge, and glacial melt water) to perform key functions such as water filtration, water storage, and biological productivity (Xue et al., 2018). However, source water dynamics and runoff processes are sensitive to changing hydroclimate conditions, and the potential implications for wetland ecosystems are poorly understood. Thus, it is necessary to build a better conceptual understanding of source water dynamics and runoff generation in Subalpine and Montane Subregions to inform management practices and best predict imminent changes in wetland ecosystems and their surrounding catchments.

The scope of this study is unique in that it provides an opportunity to compare and analyze wetland source water dynamics across a large spatial area, spanning multiple Subregions and growing seasons. Overall, we found that the spatiotemporal distribution of δ^{18}O and d-excess in source waters across all sites (Burstall Wetland, Extensive and Intensive Sites) conformed to expectations, indicating that both rain and snow are important components of recharge in the Kananaskis Valley. In Burstall Wetland, MixSIAR results revealed considerable mixing of source waters during the pre-growing season driven by snowmelt inputs to streams and groundwater. During the peak- growing season rain became the dominant driver of runoff generation to downstream water bodies, which alligned with periods of higher temperatures. This season also intersects with a period of little to no rain in July, potentially leaving Burstall Wetland vulnerable to drought or substantial water table drawdown during the summer. Results showed mixing again in downstream surface waters during the post- growing season as stream waters contributed a greater proportion, likely due to rapid flow from glacial meltwater inputs. δ^{18}O signatures from extensive and intensive sites showed similar spatiotemporal trends however, there was minimal variability within individual sites. Evaporative fluxes from extensive sites decreased with

53

increasing elevation and isotopic values became further removed from the meteoric water lines. In the Subalpine Subregion, evaporative signals were suppressed, indicating consistent seasonal inputs from snowmelt, upland runoff, rain, and glacial meltwater.

Knowledge gained from this study provides a better understanding of subalpine and montane wetland source water dynamics and influence from hydroclimate factors. Overall, subalpine wetlands have been largely underrepresented in source water partitioning and hydrologic processes literature, but are vulnerable to impacts from climate change, making results from this study important for establishing a working understanding of baseline conditions within these systems. The insights and conclusions drawn from this research will help fill gaps in our understanding of hydrometric controls on runoff generation and water usage/storage in subalpine wetland ecosystems. Lastly, the highlighted importance of snowmelt and rainfall to runoff generation will help inform future models by improving our understanding of spatiotemporal source water dynamics within ecosystems in mountainous landscapes.

4.2 Project Limitations

This study encountered some limitations that are important to address. For the source water partitioning study, the linear mixing model, MixSIAR, relies on use of stable water isotopes individually to calculate source water proportions, which, if water samples experienced evaporation would cause fractionation especially evident in δ^2H. This fractionation could cause erroneous model results. MixSIAR uses stable water isotopes combined, which eliminates the bias and error associated with calculating mixing individually. Further, source water samples (rain, snow, stream, groundwater, and surface water) for Chapter 2 (Manuscript 1) were collected over a period of 3 growing seasons (2018, 2019 & 2020), which could cause inconsistencies in results.

The contribution of glacier meltwater was not explicitly considered in this study. This could have an effect on MixSIAR computations of post-growing season calculations since the Robertson Glacier is an integral component of the Burstall Valley hydrology (Beierle et al., 2003).

The quantity of snow samples collected in this study were sparse. The relatively enriched signals of snow during the pre-growing season is likely a result of progressive seasonal isotopic enrichment that snowpacks undergo during the melting process (Taylor et al., 2001). The importance of snow and snowmelt, however, is heavily documented in the Canadian Rocky

Mountains (Fang et al., 2013; Mercer et al., 2018; Pomeroy et al., 2016; Hrach et al., 2021; Hayashi et al., 2016). In glacier-fed catchments of the Canadian Rockies, streams originate from glacial meltwater and snow that recharges aquifers during late spring (Penna et al., 2013). In wetlands, this snowmelt provides the primary source that replenishes surface water, recharges groundwater, and contributes to downstream contributions during the spring months. Melt from the seasonal snowpack is known to be the main contributor of streamflow in the eastern slopes of the Canadian Rockies (Fang and Pomeroy, 2020) and should be emphasized in future studies.

References

Adhikari, S., & Marshall, S. J. (2013). Influence of high-order mechanics on simulation of glacier response to climate change: insights from Haig Glacier, Canadian Rocky Mountains. The Cryosphere, 7(5), 1527-1541.

Ala-Aho, P., Soulsby, C., Pokrovsky, O. S., Kirpotin, S. N., Karlsson, J., Serikova, S., ... & Tetzlaff, D. (2018). Using stable isotopes to assess surface water source dynamics and hydrological connectivity in a high-latitude wetland and permafrost influenced landscape. *Journal of Hydrology*, 556, 279-293.

Beierle, B. D., Smith, D. G., & Hills, L. V. (2003). Late quaternary glacial and environmental history of the Burstall Pass area, Kananaskis Country, Alberta, Canada. *Arctic, Antarctic, and Alpine Research*, 35(3), 391-398.

Brooks, J. R., Mushet, D. M., Vanderhoof, M. K., Leibowitz, S. G., Christensen, J. R., Neff, B. P., ... & Alexander, L. C. (2018). Estimating wetland connectivity to streams in the Prairie Pothole Region: An isotopic and remote sensing approach. *Water Resources Research,* 54(2), 955-977.

Brooks, J. R., Wigington Jr, P. J., Phillips, D. L., Comeleo, R., & Coulombe, R. (2012). Willamette River Basin surface water isoscape (δ18O and δ2H): temporal changes of source water within the river. *Ecosphere*, 3(5), 1-21.

Bullock, A., & Acreman, M. (2003). The role of wetlands in the hydrological cycle. *Hydrology and Earth System Sciences*, 7(3), 358-389.

Burn, D. H. (1994). Hydrologic effects of climatic change in west-central Canada. *Journal of Hydrology*, *160*(1-4), 53-70.

Cable, J., Ogle, K., & Williams, D. (2011). Contribution of glacier meltwater to streamflow in the Wind River Range, Wyoming, inferred via a Bayesian mixing model applied to isotopic measurements. *Hydrological Processes*, 25(14), 2228-2236.

Cao, X., Wu, P., Zhou, S., Han, Z., Tu, H., & Zhang, S. (2018). Seasonal variability of oxygen and hydrogen isotopes in a wetland system of the Yunnan-Guizhou Plateau, southwest China: a quantitative assessment of groundwater inflow fluxes. *Hydrogeology journal*, 26(1), 215-231.

Carol, E., del Pilar Alvarez, M., Candanedo, I., Saavedra, S., Arcia, M., & Franco, A. (2020). Surface water–groundwater interactions in the Matusagaratí wetland, Panama. *Wetlands Ecology and Management*, 28(6), 971-982.

Clay, A., Bradley, C., Gerrard, A. J., & Leng, M. J. (2004). Using stable isotopes of water to infer wetland hydrological dynamics. *Hydrology and Earth System Sciences*, 8(6), 1164-1173.

Colvin, S. A., Sullivan, S. M. P., Shirey, P. D., Colvin, R. W., Winemiller, K. O., Hughes, R. M., ... & Eby, L. (2019). Headwater streams and wetlands are critical for sustaining fish, fisheries, and ecosystem services. *Fisheries*, 44(2), 73-91.

Cowie, R. M., Knowles, J. F., Dailey, K. R., Williams, M. W., Mills, T. J., & Molotch, N. P. (2017). Sources of streamflow along a headwater catchment elevational gradient. *Journal of Hydrology*, *549*, 163-178.

Craig, H. (1961). Standard for reporting concentrations of deuterium and oxygen-18 in natural waters. *Science*, 133(3467), 1833-1834.

Cui, J., Tian, L., Biggs, T. W., & Wen, R. (2017). Deuterium-excess determination of evaporation to inflow ratios of an alpine lake: Implications for water balance and modeling. *Hydrological Processes*, 31(5), 1034-1046.

Dansgaard, W. (1964). Stable isotopes in precipitation. *Tellus*, 16(4), 436-468.

Downing, D. J., & Pettapiece, W. W. (2006). Natural Regions Committee 2006. Natural Regions and Subregions of Alberta. Publ.

England, N., James, A. L., Chutko, K. J., Pyrce, R. S., & Yao, H. (2019). Hydrologic and water isotope characterization of a regulated Canadian Shield river basin. *Hydrological Processes*, *33*(6), 905-919.

Fang, X., & Pomeroy, J. W. (2020). Diagnosis of future changes in hydrology for a Canadian Rockies headwater basin. *Hydrology and Earth System Sciences*, 24(5), 2731-2754.

Fang, X., Pomeroy, J. W., Ellis, C. R., MacDonald, M. K., DeBeer, C. M., & Brown, T. (2013). Multi-variable evaluation of hydrological model predictions for a headwater basin in the Canadian Rocky Mountains. *Hydrology and Earth System Sciences*, 17(4), 1635-1659.

Froehlich, K., Kralik, M., Papesch, W., Rank, D., Scheifinger, H., & Stichler, W. (2008). Deuterium excess in precipitation of Alpine regions–moisture recycling. Isotopes in *Environmental and Health Studies*, 44(1), 61-70.

Fyfe, J. C., & Flato, G. M. (1999). Enhanced climate change and its detection over the Rocky Mountains. *Journal of Climate*, 12(1), 230-243.

Gat, J. R. (1996). Oxygen and hydrogen isotopes in the hydrologic cycle. *Annual Review of Earth and Planetary Sciences*, 24(1), 225-262.

Gibson, J. J., Edwards, T. W. D., Bursey, G. G., & Prowse, T. D. (1993). Estimating Evaporation Using Stable Isotopes: Quantitative Results and Sensitivity Analysis for Two Catchments in Northern Canada: Paper presented at the 9th Northern Res. Basin Symposium/Workshop (Whitehorse/Dawson/Inuvik, Canada-August 1992). *Hydrology Research*, 24(2-3), 79-94.

Gignac LD, Vitt DH, Zoltai SC, Bayley SE (1991) Bryophyte response surfaces along climatic, chemical, and physical gradients in peatlands of western Canada. *Nova Hedwigia* 53(1–2):27–71

Gleick, P. H. (1987). The development and testing of a water balance model for climate impact assessment: modeling the Sacramento basin. *Water Resources Research*, *23*(6), 1049-1061.

Gröning, M., Lutz, H. O., Roller-Lutz, Z., Kralik, M., Gourcy, L., & Pöltenstein, L. (2012). A simple rain collector preventing water re-evaporation dedicated for δ18O and δ2H analysis of cumulative precipitation samples. *Journal of Hydrology*, 448, 195-200.

Gurtz, J., Baltensweiler, A., & Lang, H. (1999). Spatially distributed hydrotope-based modelling of evapotranspiration and runoff in mountainous basins. *Hydrological processes*, 13(17), 2751-2768.

Harder, P. (2008). Hydroclimatological trends in the Kananaskis Valley. Centre for Hydrology Internal Report, University of Saskatchewan, Saskatoon.

Harpold, A. A., & Kohler, M. (2017). Potential for changing extreme snowmelt and rainfall events in the mountains of the western United States. *Journal of Geophysical Research: Atmospheres*, 122(24), 13-219.

Hayashi, M., van der Kamp, G., & Rosenberry, D. O. (2016). Hydrology of prairie wetlands: understanding the integrated surface-water and groundwater processes. *Wetlands*, 36(2), 237-254.

Hayashi, M., & Farrow, C. R. (2014). Watershed-scale response of groundwater recharge to inter-annual and inter-decadal variability in precipitation (Alberta, Canada). *Hydrogeology Journal,* 22(8), 1825-1839.

Hayashi, M., Quinton, W. L., Pietroniro, A., & Gibson, J. J. (2004). Hydrologic functions of wetlands in a discontinuous permafrost basin indicated by isotopic and chemical signatures. *Journal of Hydrology*, 296(1-4), 81-97.

Hopkinson, C., & English, M. C. (2001). Spatiotemporal variations of δ18O isotope signatures of hydrological components within a glacierised mountainous basin. In Proceedings of the 58th Eastern Snow Conference (pp. 14-18). Ottawa, Ontario, Canada.

Hrach, D. M. (2020). Quantifying the role of shade on microclimate conditions and water use efficiency of a subalpine wetland in the Canadian Rocky Mountains, Kananaskis, Alberta (Master's thesis, University of Waterloo).

Hrach, D. M., Green, A., Khomik, M., & Petrone, R. M. (2021). Analysis of growing season carbon and water fluxes of a subalpine wetland in the Canadian Rocky Mountains:

implications of shade on ecosystem water use efficiency. *Hydrological Processes*, e14425.

Hrach, D. M., Petrone, R. M., Van Huizen, B., Green, A., & Khomik, M. (2021). The Impact of Variable Horizon Shade on the Growing Season Energy Budget of a Subalpine Headwater Wetland. *Atmosphere*, 12(11), 1473.

Immerzeel, W. W., Van Beek, L. P. H., Konz, M., Shrestha, A. B., & Bierkens, M. F. P. (2012). Hydrological response to climate change in a glacierized catchment in the Himalayas. *Climatic change*, 110(3), 721-736.

Jin, S. G., Hassan, A. A., & Feng, G. P. (2012). Assessment of terrestrial water contributions to polar motion from GRACE and hydrological models. *Journal of Geodynamics*, 62, 40-48.

Juras, R., Pavlásek, J., Vitvar, T., Šanda, M., Holub, J., Jankovec, J., & Linda, M. (2016). Isotopic tracing of the outflow during artificial rain-on-snow event. *Journal of Hydrology*, 541, 1145-1154.

Kadykalo, A. N., & Findlay, C. S. (2016). The flow regulation services of wetlands. *Ecosystem services*, 20, 91-103.

Katvala, S. M. (2008). Isotope hydrology of the upper Bow River basin, Alberta, Canada (Master's thesis, University of Calgary)

Kendall, C., & Coplen, T. B. (2001). Distribution of oxygen-18 and deuterium in river waters across the United States. *Hydrological processes*, 15(7), 1363-1393.

Klein, E., Berg, E. E., & Dial, R. (2005). Wetland drying and succession across the Kenai Peninsula Lowlands, south-central Alaska. *Canadian Journal of Forest Research*, 35(8), 1931-1941.

Knowles, J. F., Harpold, A. A., Cowie, R., Zeliff, M., Barnard, H. R., Burns, S. P., ... & Williams, M. W. (2015). The relative contributions of alpine and subalpine ecosystems to the water balance of a mountainous, headwater catchment. *Hydrological Processes*, *29*(22), 4794-4808.

Kong, Y., & Pang, Z. (2016). A positive altitude gradient of isotopes in the precipitation over the Tianshan Mountains: Effects of moisture recycling and sub-cloud evaporation. *Journal of Hydrology*, 542, 222-230.

Langs, L. E., Petrone, R. M., & Pomeroy, J. W. (2020). A δ18O and δ2H stable water isotope analysis of subalpine forest water sources under seasonal and hydrological stress in the Canadian Rocky Mountains. *Hydrological Processes*, 34(26), 5642-5658.

Lee, K. S., Grundstein, A. J., Wenner, D. B., Choi, M. S., Woo, N. C., & Lee, D. H. (2003). Climatic controls on the stable isotopic composition of precipitation in Northeast Asia.

Climate Research, 23(2), 137-148.

Lee, S. Y., Ryan, M. E., Hamlet, A. F., Palen, W. J., Lawler, J. J., & Halabisky, M. (2015). Projecting the hydrologic impacts of climate change on montane wetlands. *Plos one*, 10(9), e0136385.

Le Maitre, D. C., Scott, D. F., & Colvin, C. (1999). Review of information on interactions between vegetation and groundwater.

Lessels, J. S., Tetzlaff, D., Birkel, C., Dick, J., & Soulsby, C. (2016). Water sources and mixing in riparian wetlands revealed by tracers and geospatial analysis. *Water Resources Research*, 52(1), 456-470.

Leuthold, S. J., Ewing, S. A., Payn, R. A., Miller, F. R., & Custer, S. G. (2021). Seasonal connections between meteoric water and streamflow generation along a mountain headwater stream. *Hydrological Processes*, 35(2), e14029.

Liu, Y., & Yamanaka, T. (2012). Tracing groundwater recharge sources in a mountain–plain transitional area using stable isotopes and hydrochemistry. *Journal of Hydrology*, 464, 116-126.

Lone, A., Jeelani, G., Deshpande, R. D., & Padhya, V. (2021). Estimating the sources of stream water in snow dominated catchments of western Himalayas. *Advances in Water Resources*, 155, 103995.

López-Moreno, J. I., Pomeroy, J. W., Morán-Tejeda, E., Revuelto, J., Navarro-Serrano, F. M., Vidaller, I., & Alonso-González, E. (2021). Changes in the frequency of global high mountain rain-on-snow events due to climate warming. *Environmental Research Letters*, 16(9), 094021.

Mark, B. G., & Seltzer, G. O. (2003). Tropical glacier meltwater contribution to stream discharge: a case study in the Cordillera Blanca, Peru. *Journal of glaciology*, 49(165), 271-281.

Marshall, S. J., White, E. C., Demuth, M. N., Bolch, T., Wheate, R., Menounos, B., ... & Shea, J. M. (2011). Glacier water resources on the eastern slopes of the Canadian Rocky Mountains. *Canadian Water Resources Journal*, 36(2), 109-134.

Maurya, A. S., Shah, M., Deshpande, R. D., Bhardwaj, R. M., Prasad, A., & Gupta, S. K. (2011). Hydrograph separation and precipitation source identification using stable water isotopes and conductivity: River Ganga at Himalayan foothills. *Hydrological Processes*, 25(10), 1521-1530.

McDonnell, J. J., & Beven, K. (2014). Debates—The future of hydrological sciences: A (common) path forward? A call to action aimed at understanding velocities, celerities and residence time distributions of the headwater hydrograph. *Water Resources Research*, 50(6), 5342-

5350.

Mercer, J. J. (2018). Insights into mountain wetland resilience to climate change: An evaluation of the hydrological processes contributing to the hydrodynamics of alpine wetlands in the Canadian Rocky Mountains (Doctoral dissertation, University of Saskatchewan).

Moran, T. A., Marshall, S. J., Evans, E. C., & Sinclair, K. E. (2007). Altitudinal gradients of stable isotopes in lee-slope precipitation in the Canadian Rocky Mountains. *Arctic, Antarctic, and Alpine Research*, 39(3), 455-467.

Morrison, A., Westbrook, C. J., & Bedard-Haughn, A. (2015). Distribution of Canadian Rocky Mountain wetlands impacted by beaver. *Wetlands*, *35*(1), 95-104.

Mosquera, G. M., Célleri, R., Lazo, P. X., Vaché, K. B., Perakis, S. S., & Crespo, P. (2016). Combined use of isotopic and hydrometric data to conceptualize ecohydrological processes in a high-elevation tropical ecosystem. *Hydrological Processes*, 30(17), 2930-2947.

Musselman, K. N., Lehner, F., Ikeda, K., Clark, M. P., Prein, A. F., Liu, C., ... & Rasmussen, R. (2018). Projected increases and shifts in rain-on-snow flood risk over western North America. *Nature Climate Change*, 8(9), 808-812.

Penna, D., Engel, M., Mao, L., Dell'Agnese, A., Bertoldi, G., & Comiti, F. (2014). Tracer-based analysis of spatial and temporal variations of water sources in a glacierized catchment. *Hydrology and Earth System Sciences*, 18(12), 5271-5288.

Poage, M. A., & Chamberlain, C. P. (2001). Empirical relationships between elevation and the stable isotope composition of precipitation and surface waters: considerations for studies of paleoelevation change. *American Journal of Science*, 301(1), 1-15.

Pomeroy, J. W., Stewart, R. E., & Whitfield, P. H. (2016). The 2013 flood event in the South Saskatchewan and Elk River basins: Causes, assessment and damages. *Canadian Water Resources Journal/Revue Canadienne Des Ressources Hydriques*, 41(1-2), 105-117.

Pomeroy, J. W., de Boer, D., & Martz, L. W. (2005). Hydrology and water resources of Saskatchewan (p. 25). Saskatoon: Centre for Hydrology, University of Saskatchewan.

Pu, T., He, Y., Zhu, G., Zhang, N., Du, J., & Wang, C. (2013). Characteristics of water stable isotopes and hydrograph separation in Baishui catchment during the wet season in Mt. Yulong region, south western China. *Hydrological Processes*, 27(25), 3641-3648.

Rangwala, I., & Miller, J. R. (2012). Climate change in mountains: a review of elevation-dependent warming and its possible causes. *Climatic change*, 114(3), 527-547.

Ray, A. M., Sepulveda, A. J., Irvine, K. M., Wilmoth, S. K., Thoma, D. P., & Patla, D. A. (2019). Wetland drying linked to variations in snowmelt runoff across Grand Teton and Yellowstone national parks. *Science of the Total Environment*, 666, 1188-1197.

Reynolds, J. (2020). Avian species richness elevational patterns in mountain peatlands (Master's thesis, University of Waterloo).

Rodgers, P., Soulsby, C., Waldron, S., & Tetzlaff, D. (2005). Using stable isotope tracers to assess hydrological flow paths, residence times and landscape influences in a nested mesoscale catchment. *Hydrology and Earth System Sciences*, 9(3), 139-155.

Ronnquist, A. L., & Westbrook, C. J. (2021). Beaver dams: How structure, flow state, and landscape setting regulate water storage and release. *Science of The Total Environment*, 785, 147333.

Rücker, A., Boss, S., Kirchner, J. W., & Freyberg, J. V. (2019). Monitoring snowpack outflow volumes and their isotopic composition to better understand streamflow generation during rain-on-snow events. *Hydrology and Earth System Sciences*, 23(7), 2983-3005.

Šanda, M., Vitvar, T., Kulasová, A., Jankovec, J., & Císlerová, M. (2014). Run-off formation in a humid, temperate headwater catchment using a combined hydrological, hydrochemical and isotopic approach (Jizera Mountains, Czech Republic). *Hydrological Processes*, 28(8), 3217-3229.

Scanlon, R. S. (2017). Modeling mass balance at Robertson Glacier, Alberta, Canada 1912-2012 (Doctoral dissertation, Montana State University-Bozeman, College of Letters & Science).

Shi, Y., Jia, W., Zhu, G., Ding, D., Yuan, R., Xu, X., ... & Xiong, H. (2021). Hydrogen and Oxygen Isotope Characteristics of Water and the Recharge Sources in Subalpine of Qilian Mountains, China. *Polish Journal of Environmental Studies*, 30(3).

Shi, M., Wang, S., Argiriou, A. A., Zhang, M., Guo, R., Jiao, R., ... & Zhou, S. E. (2019). Stable Isotope Composition in Surface Water in the Upper Yellow River in Northwest China. *Water*, 11(5), 967.

Smith, C. D. (2008). The relationship between monthly precipitation and elevation in the Alberta foothills during the foothills orographic precipitation experiment. In Cold Region Atmospheric and Hydrologic Studies. The Mackenzie GEWEX Experience (pp. 167-185). *Springer*, Berlin, Heidelberg.

Soulsby, C., Birkel, C., Geris, J., Dick, J., Tunaley, C., & Tetzlaff, D. (2015). Stream water age distributions controlled by storage dynamics and nonlinear hydrologic connectivity: Modeling with high-resolution isotope data. *Water Resources Research*, 51(9), 7759-7776.

Stewart, R. E., Bachand, D., Dunkley, R. R., Giles, A. C., Lawson, B., Legal, L., Miller, S. T., Murphy, B. P., Parker, M. N., Paruk, B. J., and Yau, M. K., (1995): Winter storms over Canada. *Atmosphere-Ocean*, 33(2): 233–247.

Stock, B. C., & Semmens, B. X. (2016). Unifying error structures in commonly used biotracer mixing models. *Ecology*, 97(10), 2562-2569.

Stock, B. C., Jackson, A. L., Ward, E. J., Parnell, A. C., Phillips, D. L., & Semmens, B. X. (2018). Analyzing mixing systems using a new generation of Bayesian tracer mixing models. *PeerJ*, 6, e5096.

Tague, C., & Dugger, A. L. (2010). Ecohydrology and climate change in the mountains of the Western USA–A review of research and opportunities. *Geography Compass*, 4(11), 1648-1663.

Taylor, S., Feng, X., Kirchner, J. W., Osterhuber, R., Klaue, B., & Renshaw, C. E. (2001). Isotopic evolution of a seasonal snowpack and its melt. *Water Resources Research*, 37(3), 759-769.

Tazioli, A., Cervi, F., Doveri, M., Mussi, M., Deiana, M., & Ronchetti, F. (2019). Estimating the isotopic altitude gradient for hydrogeological studies in mountainous areas: are the low-yield springs suitable? insights from the Northern Apennines of Italy. *Water*, 11(9), 1764.

Thériault, J. M., Hung, I., Vaquer, P., Stewart, R. E., & Pomeroy, J. W. (2018). Precipitation characteristics and associated weather conditions on the eastern slopes of the Canadian Rockies during March–April 2015. *Hydrology and Earth System Sciences*, 22(8), 4491-4512.

Toop D, de la Cruz NN (2002) Hydrogeology of the Canmore corridor and northwestern Kananaskis Country. Alberta, Alberta Environment, Hydrogeology Section, Edmonton, AB

Wassenaar, L. I., Athanasopoulos, P., & Hendry, M. J. (2011). Isotope hydrology of precipitation, surface and ground waters in the Okanagan Valley, British Columbia, Canada. *Journal of Hydrology*, 411(1-2), 37-48.

Whitfield, P. H. (2014). Climate station analysis and fitness for purpose assessment of 3053600 Kananaskis, Alberta. *Atmosphere-Ocean*, 52(5), 363-383.

Whitfield, C. J., Aherne, J., Gibson, J. J., Seabert, T. A., & Watmough, S. A. (2010). The controls on boreal peatland surface water chemistry in Northern Alberta, Canada. *Hydrological Processes*, 24(15), 2143-2155.

Windell, J. T., & Segelquist, C. (1986). An ecological characterization of Rocky Mountain montane and subalpine wetlands (Vol. 86, No. 11). *Fish and Wildlife Service*, US

Winter, S. G. (2000). The satisficing principle in capability learning. *Strategic management journal*, 21(10-11), 981-996.

Winter, T. C. (1999). Relation of streams, lakes, and wetlands to groundwater flow systems. *Hydrogeology Journal*, 7(1), 28-45.

Woo, M. K., & Young, K. L. (2006). High Arctic wetlands: their occurrence, hydrological characteristics and sustainability. *Journal of Hydrology*, 320(3-4), 432-450.

Xue, Z., Lyu, X., Chen, Z., Zhang, Z., Jiang, M., Zhang, K., & Lyu, Y. (2018). Spatial and temporal changes of wetlands on the Qinghai-Tibetan Plateau from the 1970s to 2010s. *Chinese Geographical Science*, 28(6), 935-945.